Received: 15 October 2023 | Revised: 2 February 2024 | Accepted: 7 February 2024

DOI: 10.1002/ar.25414

SPECIAL ISSUE ARTICLE

The Anatomical Record WILEY

The Sima de los Huesos thorax and lumbar spine: Selected traits and state-of-the-art

Asier Gómez-Olivencia[1,2,3] | **Juan Luis Arsuaga**[3,4]

[1]Dept. Geología, Facultad de Ciencia y Tecnología, Universidad del País Vasco/Euskal Herriko Unibertsitatea (UPV/EHU), Leioa, Spain

[2]Sociedad de Ciencias Aranzadi, Donostia-San Sebastián, Spain

[3]Centro UCM-ISCIII de Investigación sobre Evolución y Comportamiento Humanos, Madrid, Spain

[4]Departamento de Geodinámica, Estratigrafía y Paleontología, Facultad de Ciencias Geológicas, Universidad Complutense de Madrid, Madrid, Spain

Correspondence
Asier Gómez-Olivencia, Dept. Geología, Facultad de Ciencia y Tecnología, Universidad del País Vasco/Euskal Herriko Unibertsitatea (UPV/EHU), Barrio Sarriena s/n, 48940 Leioa, Spain.
Email: asier.gomezo@ehu.eus

Funding information
Ministerio de Ciencia, Innovación y Universidades, Grant/Award Numbers: PGC2018-093925-B-C33, PID2021-122355NB-C31; Ramón y Cajal fellowship, Grant/Award Number: RYC-2017-22558; Fundación Atapuerca; Junta de Castilla y León

Abstract

Information on the evolution of the thorax and lumbar spine in the genus *Homo* is hampered by a limited fossil record due to the inherent fragility of vertebrae and ribs. Neandertals show significant metric and morphological differences in these two anatomical regions, when compared to *Homo sapiens*. Thus, the important fossil record from the Middle Pleistocene site of Sima de los Huesos (SH) not only offers important information on the evolution of these anatomical regions within the Neandertal lineage but also provides important clues to understand the evolution of these regions at the genus level. We present the current knowledge of the costal skeleton, and the thoracic and lumbar spine anatomy of the hominins found in Sima de los Huesos compared to that of Neandertals and modern humans. The current SH fossil record comprises 738 vertebral specimens representing a minimum of 70 cervical, 95 thoracic and 47 lumbar vertebrae, 652 rib fragments representing a minimum of 118 ribs, and 26 sternal fragments representing 4 sterna. The SH hominins exhibit a morphological pattern in their thorax and lumbar spine more similar to that of Neandertals than to that of *H. sapiens*, which is consistent with the phylogenetic position of these hominins. However, there are some differences between the SH hominins and Neandertals in these anatomical regions, primarily in the orientation of the lumbar transverse processes and in the robusticity of the second ribs. The presence of some but not all of the suite of Neandertal-derived features is consistent with the pattern found in the cranium and other postcranial regions of this population.

KEYWORDS

lumbar vertebrae, ribs, spino-pelvic posture, sternum, thoracic vertebrae

1 | INTRODUCTION

The thorax and the lumbar spine are important anatomical regions because they provide important information about body size and locomotion, among other things. The thorax connects the neck to the lumbar spine, provides attachment for muscles related to the movement of the head, trunk, and upper limbs, as well as muscles related to the breathing, and protect important organs such as the heart and the lungs (Kapandji, 1974). The

Abbreviations: LL, lumbar lordosis; SH, Sima de los Huesos.

lumbar spine connects the thorax to the pelvis and provides attachment for muscles involved in the movement of the trunk, lower limb and breathing, among others (Kapandji, 1974). Despite extensive variation, when compared to cercopithecoids, extant hominoids show significant differences in their thoracic morphology, related to an enhanced ability to maintain an erect trunk (orthogrady) (Aiello & Dean, 1990; Preuschoft, 2004; Schultz, 1961, and references therein).

Integration studies on the modern human vertebral column have shown that the potential to evolve is different depending on the region. In fact, the lowermost thoracic (T10-T12) and the lumbar vertebrae are more evolvable than the cervical and the rest of the thoracic vertebrae. Additionally, the atlas (C1) and the fifth lumbar vertebra (L5) show the lowest values of integration compared to the rest of the vertebral elements, and the thoracic vertebrae, on the contrary, display the highest magnitudes of integration (Arlegi et al., 2020). Moreover, a more complex integration model has recently been proposed in the modern human torso with the highest covariation between lowest rib levels and the ilia (Torres-Tamayo et al., 2018). In fact, the covariation between pelvic morphology and the thorax can allow for the prediction of the latter based on the former (Torres-Tamayo et al., 2020).

Vertebrae and ribs are metameric elements which makes their anatomical determination difficult, especially in cases in which there is a high anatomical similarity between adjacent elements, which happens in most of the thoracic vertebrae (T2-T9), most lumbar vertebrae (L1-L4) and most ribs (from the 3rd to the 10th). Vertebrae and ribs are also fragile elements, and therefore, their fossil record is relatively scarce, especially when compared with other anatomical regions such as teeth or mandibles. The difficulty to amass reasonable comparative samples in the museum collections and a traditional greater interest in other anatomical regions such as crania, mandibles, teeth, or long bones has traditionally relegated the study of both the thoracic (and to a lesser extent lumbar) vertebrae and ribs of important fossil hominins, when present, to smaller chapters within large monographs (e.g., Heim, 1976; Trinkaus, 1983).

However, there have been interesting debates based on these anatomical regions that are related to important aspects of the study of human evolution such as the evolution of the body size and shape, and locomotion. On one hand, there is still an ongoing debate about the shape of the autralopith thorax (Schmid, 1983; Schmid et al., 2013; contra Haile-Selassie et al., 2010), and the size and shape of the Neandertal thorax has been an object of speculation since the first findings of Neandertal ribs. In fact, Neandertal thorax has been referred as "hyper-barrel chest" or "bell-shaped" (e.g., Sawyer & Maley, 2005; Weinstein, 2008). On the other hand, the role of the lumbar morphology in bipedalism (Robinson, 1972; Sanders, 1998), and the variation in lumbar curvature within Late Pleistocene hominins have been the subject of debate (e.g., Been et al., 2012, 2014; Gómez-Olivencia et al., 2017; contra Haeusler et al., 2019).

In the last 40 years, the fossil record has increased and new techniques have been applied to the study of the thorax and the lumbar spine in genus *Homo*. Both the description of new fossils and the review of older fossils are providing new insights into the evolution of these anatomical regions in the genus *Homo* (e.g., Carretero et al., 1999; Franciscus & Churchill, 2002; Meyer, 2005; Gómez-Olivencia et al., 2009, 2010, 2017, 2018, 2019; Been et al., 2010, 2012, 2014, 2017; Haeusler et al., 2011; Arlegi et al., 2017; Bastir et al., 2015, 2020; Bastir, García Martínez, et al., 2017; García-Martínez et al., 2017; Williams et al., 2017).

In this scenario, the Middle Pleistocene site of Sima de los Huesos, with an age of approximately 430 thousand years, has yielded a large collection of fossil hominin remains, including elements of the spine and thorax (Arsuaga et al., 2014, 2015). The vertebrae and ribs found at this site provides the opportunity to understand: (a) the evolution of the thorax and the lumbar spine within the Neandertal lineage, owing to their phylogenetic affinities between Neandertals and the Sima de los Huesos (SH) hominins (Arsuaga et al., 2014, 2015; Martínez & Arsuaga, 1997; Meyer et al., 2016); and (b) the evolution of these two anatomical regions within the genus *Homo*.

The objective of this work is to present the current knowledge of the anatomy of the thorax (costal skeleton, thoracic spine and sternum) and lumbar spine of the hominins found in Sima de los Huesos compared to that of Neandertals and modern humans, and when possible to earlier members of genus *Homo*. The perceived differences will be discussed within an evolutionary and biomechanical framework.

1.1 | The thorax and lumbar spine fossil record in genus *Homo* in the Lower and Middle Pleistocene

In order to fully understand the morphological features of the thorax and lumbar spine of the SH hominins, here we provide a selected account of other fossil hominins from the Lower and Middle Pleistocene.

For the genus *Homo*, the oldest thoracic, lumbar and costal remains are the *Homo erectus* remains found in Dmanisi (Georgia) with an age of approximately 1.8 million years (Ma) (Lordkipanidze et al., 2007; Meyer, 2005; Meyer & Williams, 2019, and references therein). Of the five vertebrae, associated with the adolescent cranium

D2700, two of them are thoracic vertebrae: the third thoracic (T3) vertebra D2721 and the T11 D2715, and one of them is a lumbar vertebra: the L2 D2672. The Dmanisi vertebrae belonged to a small-bodied hominin but they show key-changes such as larger surfaces of the vertebral body relative to earlier small-bodied hominins that allowed efficient long-range travel (Meyer, 2005). Additionally, Meyer (2005) underscored that the Dmanisi hominins exhibit a fully modern spinal cord size and shape. Dmanisi has also yielded four costal remains: three remains belonging to a subadult individual (D2716/D2855, right/left first rib; D2717, eleventh rib) and one belonging to a large adult individual (D4063, right second rib) (Lordkipanidze et al., 2007). However, these remains are only listed, and to our knowledge, no detailed morphometric study has been performed.

The immature individual KNM-WT 15000 (*Homo erectus/ergaster*; 1.5 Ma) preserves 10 out of the 12 thoracic vertebrae and all five lumbar vertebrae (Haeusler et al., 2002, 2011). However, the number of lumbar vertebrae assigned to this skeleton has been the subject of debate (Brown et al., 1985; Latimer & Ward, 1993; Haeusler et al., 2002, 2011). This debate has its origin on the absolute position of the transitional vertebra (the vertebra in which the orientation of the articular facets changes from a more "thoracic-like" orientation to a "lumbar-like" orientation; Williams, 2012) and the number of post-transitional vertebrae on this skeleton. There is now a considerable consensus on the position of this vertebra on the 18th vertebrae (T11) and the presence of six post-transitional vertebrae, which parallels the pattern found in all the australopiths in which this feature has been observed (Haeusler et al., 2002; Ward et al., 2017; Williams & Meyer, 2019, and references therein). Based on the lumbar vertebrae, Been et al. (2012) calculated the lumbar lordosis of the KNM-WT 15000 juvenile *H. erectus* to be 45°, which is below but close (−0.55 standard deviations) to their modern human comparative sample mean (51.1 ± 11.0). This lumbar lordosis value is similar to that obtained for the BSN49/P27 adult pelvis from Gona (43–48°) based on its pelvic incidence (Been et al., 2014). The costal skeleton of this specimen was described in detail by Jellema et al. (1993). The review of the anatomical features conducted by these scholars "demonstrates that the rib cage of this specimen was in almost all respects indistinguishable from those of modern humans" (Jellema et al., 1993: 324). It should be noted that the framework of this work was dichotomical, trying to ascertain "whether these early hominids already had the 'barrel-shaped' thorax typical of humans or whether they still retained the anthropoid configuration, or 'funnel-shaped' thorax, we now associate with chimpanzees" (Jellema et al., 1993: 294). Haeusler et al. (2011) presented two dozen rib fragments that they previously identified while browsing through the boxes containing the KNM-WT 15000 skeleton at the National Museums of Kenya, Nairobi. These findings led Haeusler et al. (2011) to a rearrangement of the ribs of this individual resulting in a more symmetrical rib cage that refuted previous claims for idiopathic or congenital scoliosis (Latimer & Ohman, 2001). Based on this new anatomical determination of the costal skeleton, and using virtual anthropology and geometric morphometric methods in order to infer the morphology of the missing elements, Bastir et al. (2020) performed a 3D virtual reconstruction of the thorax of this individual. This study demonstrated that KNM-WT 15000 had a short, mediolaterally wide and anteroposteriorly deep thorax that differs considerably from the much antero-posteriorly shallower thorax of *Homo sapiens*, and is more similar to other fossil hominins, such as the reconstruction of the Kebara 2 Neandertal thorax performed by Gómez-Olivencia et al. (2018).

Regarding the late Early Pleistocene *Homo antecessor* thoracic and lumbar fossil record, Carretero et al. (1999) indicate the presence of a fragment of subadult thoracic vertebral body (ATD6-74), a fragmentary neural arch of a thoracic vertebra (ATD6-80) and a fragmentary neural arch of a lumbar vertebra that preserves a fairly complete spinous process (ATD6-45), found in 1995. The fragmentary and/or immature status of these remains precluded a metric comparative analysis for these remains (Carretero et al., 1999). These scholars also provided an inventory of the eight ribs found in 1995 at the TD6 level but no comparative study was performed. Later, Gómez-Olivencia et al. (2010) provided an updated inventory that included one rib found in more recent excavations, a new assessment of the anatomical position and a comparative metric study. With the available fossil record, Gómez-Olivencia et al. (2010) could neither confirm nor reject the hypothesis that *H. antecessor* had a large thorax, as suggested by other skeletal elements, such as clavicles.

The partial skeleton from Jinniushan (People's Republic of China), dated to around 260 thousand years preserves five thoracic vertebrae and two left ribs (a second and a 5th or 6th) (Lü, 1990). To our knowledge, these remains have not been published in detail.

In this work, the fossil remains from *Homo floresiensis* (Morwood et al., 2005) and *Homo naledi* (Hawks et al., 2017; Williams et al., 2017) have not been taken into account due to their general differences in size with SH and the fact that they are not closely related phylogenetically.

1.2 | The thorax and lumbar spine in *Homo neanderthalensis* compared to *H. sapiens*

1.2.1 | The thoracic kyphosis and the lumbar lordosis

Despite the presence in the Neandertal fossil record of several partial to complete thoracic spines, to our knowledge, only that of Kebara 2 is complete enough to attempt the reconstruction of the thoracic kyphosis. Been et al. (2017) calculated a thoracic kyphosis of 44° based on the formula by Goh et al. (1999) for male individuals ($y = 297.114–272.31 \times x$). This value is close, but slightly below the modern human mean provided by different authors (e.g., 48°, Gelb et al., 1995; 50°, Goh et al., 1999; 50°, Jackson & Hales, 2000). New fossils and the application of other methodologies will allow testing whether this value is representative for Neandertals, and will allow interpretations of the variation in this region.

Based on the wedging of the lumbar vertebrae, Boule (1911–1913) suggested a lower degree of lordosis in Neandertals more than 100 years ago. He interpreted this feature to be an intermediate state between apes and modern humans (Boule, 1911–1913). Weber and Pusch (2008) stated that a "kyphotic lumbar spine is the natural anatomy" for two other Neandertal male individuals (Kebara 2 and Shanidar 3). Based on the relationship between lumbar lordosis and the orientation of the inferior articular processes relative to vertebral bodies, Been et al. (2012) calculated a lumbar lordosis angle of 29° ± 4 for Neandertals based on the lumbar spines of Shanidar 3, Kebara 2 and La Chapelle-aux-Saints 1. This value for Neandertals is significantly below modern and fossil *H. sapiens* (51° ± 11 and 54° ± 14, respectively). Based on the relationship between the orientation of the sacrum (pelvic incidence) and lumbar lordosis (LL), Been et al. (2014) measured the pelvic incidence of Kebara 2 and estimated the lumbar lordosis to be 29° or 36°, depending on the regression equation used. More recently, based on the pelvic incidence, Haeusler et al. (2019) estimated the lumbar lordosis of the La Chapelle-aux-Saints 1 individual to be 51°, similar to the *H. sapiens* mean. Additionally, Williams et al. (2022) compared the values of vertebral body wedging and angulation of the articular processes (both significantly related to lumbar lordosis) of two Neandertal individuals (Kebara 2 and Shanidar 3; although additional individual Neandertal vertebrae were also studied) to a large sample of pre-industrial and post-industrial *H. sapiens* populations. The pre-industrial sample showed values indicative of a lower degree of lordosis than the post-industrial samples, and in both cases, there was a significant sexual dimorphism, with female individuals being more lordotic than male individuals within the same population. In this comparison, the Neandertal sample showed values that were still smaller than the preindustrial male sample, but not significantly different. In sum, while there is still some debate, and interpretations are based on a reduced number of individuals, traditionally regarded as males, Neandertals seem to have shown more vertically oriented sacra and less curved spinal curvatures than modern humans.

1.2.2 | The morphology of the Neandertal thoracic and lumbar vertebrae

Both the thoracic and the lumbar vertebrae of Neandertals show significant differences when compared to modern humans. In the upper thoracic spine, the canal transverse diameter of the second thoracic vertebra (T2) in Neandertals is significantly larger than in modern humans (Gómez-Olivencia, Couture-Veschambre, et al., 2013), which has been related to the larger transverse dimensions of the canal in the cervical spine (Gómez-Olivencia, Been, et al., 2013). In the case of the central-lower regions, the transverse processes are oriented more dorsally and cranially than in modern humans; and the spinous processes are oriented more horizontally (Bastir, García Martínez, et al., 2017). Dorsally oriented transverse processes in the mid- to lower thoracic spine would be related to a more invaginated spine into the thorax (Gómez-Olivencia et al., 2018). It is possible that the orientation of the spinous processes in the thoracic spine is a by-product of the more invaginated spine into the thorax (Gómez-Olivencia et al., 2015).

Neandertal lumbar vertebrae show many differences that distinguish them from modern humans, but not all the vertebrae differ in the same way (Been et al., 2010; Gómez-Olivencia et al., 2017). First, Neandertals show a relatively high prevalence of lumbar ribs (Kebara 2 and Shanidar 3). Based on the same individuals, Neandertals show significantly longer transverse processes in L4 and L5, and based on Kebara 2, the only Neandertal individual that preserves the transverse processes of all the lumbar vertebrae, the maximum length of the transverse processes is reached at L4 and not L3, as in modern humans. Additionally, Neandertals show more laterally oriented transverse processes in L2-L4, and, at least in L1-L3, transverse processes are also more vertically oriented. Finally, L4 and L5 show dorso-ventrally large canals, resulting in longer laminae, oriented with more acute angles between them (Been et al., 2010; Gómez-Olivencia et al., 2017).

TABLE 1 Inventory of the most complete adult thoracic vertebrae from Sima de los Huesos.

Anatomical position	Label	Field label	Age-at-death	Description	Figure
T1	VT2	AT-1153 + AT-2755	Adult	Very complete vertebra that lacks the transverse processes and the pedicles, articular facets and part of the lamina from the left side.	–
T1	VT12	AT-3342 + AT-3343 + 3702	Young adult	Nearly complete vertebra that only lacks the tip of the left transverse process.	Figure 1
T1	VT10	AT-3009	Adult	Nearly complete vertebra that only lacks the spinous process	Figure 1
T1	–	AT-3351	Adult	Partial vertebra: left half of the vertebral body and pedicle, transverse process, articular facets and part of the lamina from the left side.	Figure 1
T2?	VT16	AT-2464 + AT-2602 + AT-2617 + AT-3977	Adult	Nearly complete vertebra that only lacks the left half of the vertebral body	–
T2?	VT15	AT-3707 + AT-3726	Adult	Nearly complete vertebra that lacks the tips of both transverse processes.	–
T3?	VT18	AT-3333 + AT-3352 + AT-3708 + AT-3709 + AT-3957	Adult	Complete vertebra.	–
T3-T4	VT24	AT-3328 + AT-3350	Young adult	Nearly complete vertebra that only lacks the left transverse process and the tip of the spinous process.	–
T3-T5	VT37	AT-1233 + AT-3966 + AT-4880 + AT-5924	Adult	Very complete vertebra that lacks the ventral two thirds of the vertebral body, and the left transverse process.	–
T3-T5	VT35	AT-6792 + AT-6797	Adult	Very complete vertebra that lacks both upper articular facets, the complete left and part of the right transverse processes, and the tip of the spinous process.	–
T3-T6	VT27	AT-1135 + AT-4008	Adult	Very complete vertebra that lacks the transverse processes, the right upper articular facet and the tip of the spinous process.	–
T4-T5	VT19	AT-3710 + AT-3715	Adult	Nearly complete vertebra that only lacks the tip of the spinous process.	Figure 2
T4-T6	VT38	AT-1134 + AT-4021	Adult	Partial vertebra that preserves the vertebral body and the pedicle, articular facets and lamina from the right side.	–
T4-T7	VT22	AT-2583 + AT-2598 + AT-3390 + AT-6111	Adult	Nearly complete vertebra that lacks the transverse processes and part of the left upper articular facet.	–
T5-T6	VT30	AT-4198 + AT-4199	Young adult	Nearly complete vertebra that lacks the transverse process and upper articular facet from the left side and the spinous process.	–
T5-T6	VT23	AT-2634 + AT-3329 + AT-3348 + AT-3703	Adult	Nearly complete vertebra that lacks the tip of the right transverse process and the transverse process and upper articular facet from the left side.	–
T6-T7	VT21	AT-3334 + AT-3353	Adult	Nearly complete vertebra that only lacks the tip of both transverse processes and the tip of the spinous process.	–
T7-T8	VT28	AT-3347 + AT-3976	Adult	Partial vertebra that preserves the vertebral body, the pedicles, the upper articular facets, the laminae and the left lower articular facet.	–

(Continues)

TABLE 1 (Continued)

Anatomical position	Label	Field label	Age-at-death	Description	Figure
T7-T8	VT17	AT-3331 + AT-3344 + 3719	Adult	Nearly complete vertebra that lacks the tips of both transverse processes.	Figure 2
T8-T9	VT31	AT-1707 + AT-2595 + AT-2702 + AT-2859	Adult	Nearly complete vertebra that lacks the pedicle and upper facet from the left side. The vertebral body is partially eroded.	–
T8-T9	VT20	AT-3330 + AT-3720 + AT-3721 + AT-3983 + AT-4886	Adult	Very complete vertebra that lacks the transverse process and part of the lower articular facet from the right side, the tip of the left transverse process, and the tip of the spinous process.	–
T10?	VT9	AT-2597 + AT-2677 + AT-2680 + AT-2694	Adult	Nearly complete vertebra that only lacks the transverse processes.	–
T11	VT36	AT-6678 + AT-6679	Adult	Nearly complete vertebra that only lacks the left transverse process.	Figure 2
T12	VT6	AT-1794	Adult	Complete vertebra.	Figure 3
T12	VT29	AT-3842 + AT-3844 + AT-3845 + AT-3846 + AT-3847 + AT-6182 + AT-6195 + AT-6230	Adult	Nearly complete vertebra that only lacks the transverse process and the lower articular facet from the left side.	Figure 3

1.2.3 | The costal skeleton, the sternum and the thorax as a whole

Based on a limited number of complete ribs (Kebara 2 and Tabun C1), when compared to modern humans, Neandertals show uppermost and lowermost ribs similar in arc length, but mid-thoracic ribs with larger arc dimensions. Mid-thoracic ribs also display large maximum diameters of the sternal end and larger distances between the tubercle and the iliocostal line. Gómez-Olivencia (2015) suggests that Neandertals tend to show larger posterior angles, with larger chords and subtenses, but they seem to scale following the modern human pattern. Regarding the shaft thickness, Neandertal ribs are also thicker than modern industrial populations in many instances (e.g., Kebara 2, La Chapelle-aux-Saints 1, Shanidar 3) (Franciscus & Churchill, 2002; García-Martínez, Radovčić, et al., 2018; Gómez-Olivencia, 2015; Gómez-Olivencia et al., 2009). Using geometric morphometrics, Bastir et al. (2015) confirmed the perception that Neandertal first ribs are less curved than in modern human, and suggested a relationship between the morphology of the first rib and the whole thorax.

Due to their fragility, Neandertal sterna are rare in the fossil record. The Neandertal manubrium has been described as similar to that of modern humans based on the Regourdou 1 individual (Vallois & de Félice, 1976). However, Neandertals seem to have long mesosterna, which has been related to a larger thorax size (Gómez-Olivencia et al., 2012). In any case, these assessments are based only on a small sample of fossil remains.

Gómez-Olivencia et al. (2018) published the reconstruction of the thorax of the Kebara 2 (K2) individual using virtual anthropology techniques. While the overall morphology is significantly different from modern humans, the overall size of the K2 thorax, based on centroid size, was not larger than modern humans, as has been previously proposed, likely due to the smaller cranio-caudal dimension of the thoracic spine. However, the reconstructed thorax of Kebara 2 shows a large medio-lateral dimension which has been related to the wide transverse dimension of the pelvis of this individual. Additionally, it was possible to observe a more invaginated spine into the thorax, which is related to the perceived differences in the orientation of the transverse processes of the thoracic spine (see above) and which could probably explain the differences in the length between the tubercle and the posterior angle. Finally, in lateral view, ribs show a more straight orientation than in modern humans. Modern humans with wider lower thoraces (as in K2) tend to have larger respiratory capacities (Bastir, García-Martínez, et al., 2017; García-Martínez et al., 2016), which would be in agreement with estimations done for this individual based on isolated ribs (García-Martínez, Torres-Tamayo, et al., 2018). The recent assessment of the thorax of Neandertal perinatal individuals under 5 years of age suggests that the Neandertal

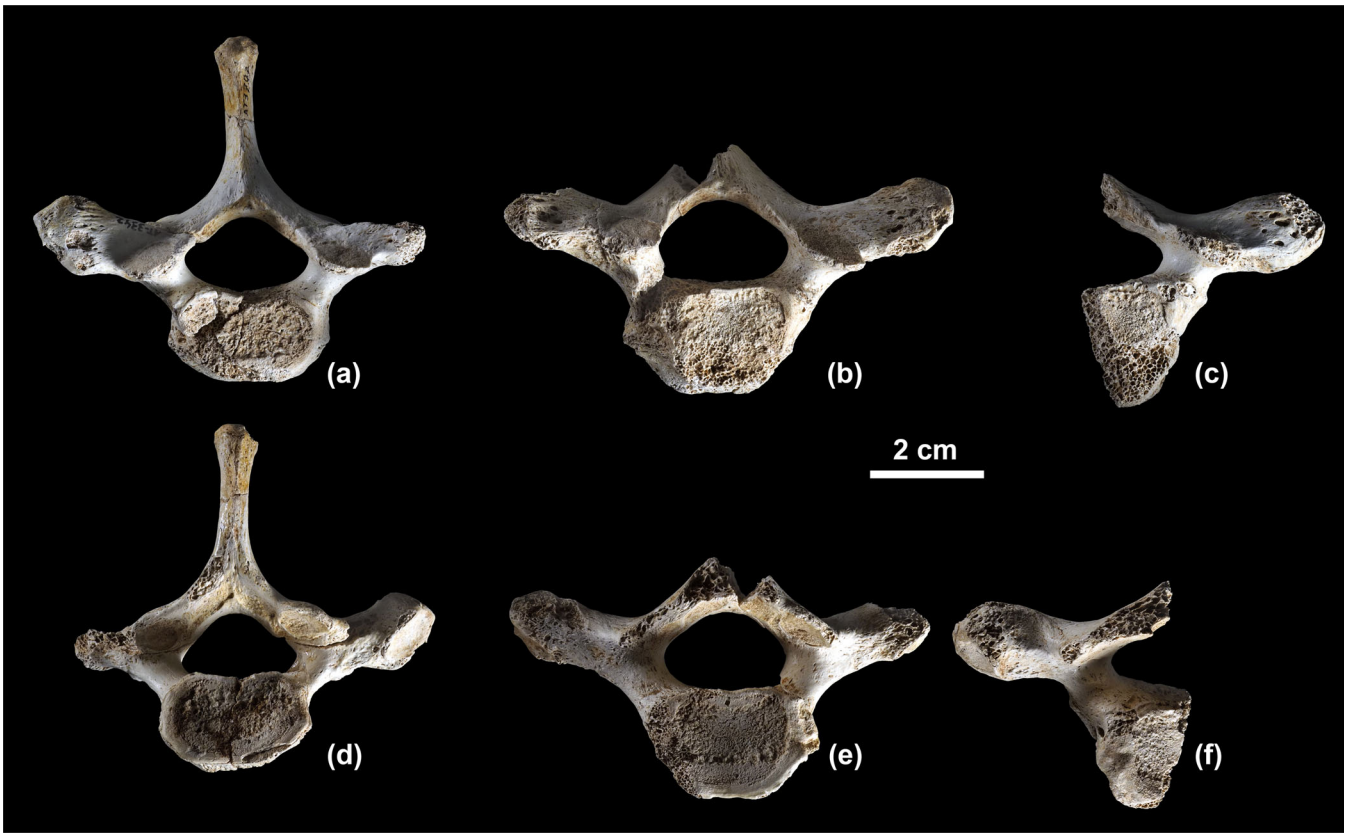

FIGURE 1 Most complete first thoracic vertebrae from Sima de los Huesos. Cranial (a) and caudal (d) views of VT12. Cranial (b) and caudal (e) views of VT10. Cranial (c) and caudal (f) views of AT-3351.

thorax morphology was different from that of modern humans, even at birth (García-Martínez et al., 2020).

2 | MATERIALS AND METHODS

2.1 | SH sample

Since 1976, SH has yielded more than 7000 human fossil remains. Of these, 335 fragments correspond to thoracic vertebrae, 175 to lumbar vertebrae, 652 to ribs and 26 to sternum (see also Sala et al., 2024). In this study, only selected traits in adult individuals are studied.

The labeling of the SH vertebrae is somehow different from that used for other skeletal remains from the same site (see Appendix 1 by Gómez-Olivencia et al., (2007); Gómez-Olivencia & Arsuaga, 2024). Apart from one or multiple "AT-" + inventory number, which is the field label, the most complete vertebrae also have another label. They are labeled with a "V" (for vertebra) and in this case, "T" for thoracic or "L" for lumbar and an Arabic number which indicates the inventory number. Because this might be confusing with the anatomical position, the latter can be included between parentheses afterwards. For example, VT10(T1) is a first thoracic vertebra while VT6(T12) is a twelfth thoracic vertebra.

In the case of the case of the most complete ribs, they are labeled with "Co" for "*costilla*" (rib in Spanish) and "*costa*" (rib in latin) and an Arabic number which indicates the inventory number (Gómez-Olivencia, 2009). Afterwards, the anatomical position and side of said rib are indicated parenthetically. For example, Co1(1L) is a first rib from the left side, while Co2(12L) is a twelfth rib from the left side.

2.2 | Comparative samples

The recent modern human comparative sample is composed of adult European males ($n = 41$), Euro American males ($n = 32$) and Euro American females ($n = 35$). The European male sample was temporarily housed at the University of Burgos (Burgos, Spain) where the sample was measured. Regarding the Euro American sample, 35 female and 26 male individuals derive from the Hamann-Todd collection (Cleveland Museum of Natural History, USA) while 6 male individuals derive from the University of Iowa (Iowa City, USA).

FIGURE 2 Selected very complete thoracic vertebrae from Sima de los Huesos). Cranial (a), caudal (b) and left lateral (c) views of the VT19(T4-T5). Cranial (d), caudal (e) and left lateral (f) views of the VT17(T7-T8). Cranial (g), caudal (h) and left lateral (i) views of the VT 36(T10).

2.3 | Methods

The metric variables have been defined elsewhere (Gómez-Olivencia et al., 2010, 2017, 2019; Gómez-Olivencia, Couture-Veschambre, et al., 2013). Measurements on bones were taken using digital calipers. Selected SH and Neandertal individuals were compared to our modern comparison sample using *z*-scores. Significant values,

FIGURE 3 Most complete twelfth thoracic vertebrae (T12) from Sima de los Huesos. Cranial (a), caudal (b) and left lateral (c) views of the VT6. Cranial (d), caudal (e) and left lateral (f) views of the VT29. Cranial view (g) of the reconstruction using mirror images and amending the asymmetry of the spinous process of VT29 articulated with the last rib Co5(12R).

TABLE 2 Dimensions (in mm) of selected vertebral measurements of the most complete first thoracic (T1) vertebrae from Sima de los Huesos compared to both Neandertals and to the summary statistics of the recent human sample, and results of the *z*-score analysis between the fossil sample and recent humans.[a]

Variable	Sima de los Huesos		Neandertals			Modern humans		
Individual/Label/Sex	VT10	VT12	Kebara 2	La Chapelle-aux-Saints 1	La Ferrassie 1	European males	Euroamerican males	Euroamerican females
Maximum dorso-ventral diameter (MaxDVDi)		61.6				60.69 ± 2.43 (54.4–66.2) $n = 33$	63.14 ± 2.54 (58.9–67.9) $n = 27$	57.24 ± 2.46 (53.1–61.9) $n = 32$
Maximum transverse diameter (MaxTrDi)	(77.5)	(75.0)	79.9			74.56 ± 3.05 (69.6–80.4) $n = 32$	77.27 ± 3.49 (70.1–83.5) $n = 27$	70.15 ± 3.52 (64.1-76.3) $n = 32$
Canal dorso-ventral diameter (M10)	14.8	13.4	15.3	15.4		15.20 ± 1.00 (12.5–17.7) $n = 37$	14.82 ± 1.20 (12.1–17.0) $n = 28$	14.42 ± 0.81 (12.2–15.6) $n = 32$
Canal transverse diameter (M11)	22.5	21.2	22.5	22.5	22.5	21.15 ± 1.14 (19.2–24.8) $n = 37$	21.40 ± 1.55 (18.8–26.1) $n = 28$	20.61 ± 1.28 (18.6–23.0) $n = 32$
Spinous process: maximum length (M13)		35.8				36.22 ± 2.56 (30.1–43.2) $n = 32$	37.52 ± 2.70 (31.5–42.0) $n = 27$	33.38 ± 2.38 (29.1–37.9) $n = 32$

[a]Values in parentheses are estimated. The z-score analysis has not yielded any significant difference between the fossil remains and the modern human comparative samples.
Source: Data from Gómez-Olivencia (2009).

TABLE 3 Dimensions (in mm) of selected vertebral measurements of the most complete twelfth thoracic (T12) vertebrae from Sima de los Huesos compared to both Neandertals and to the summary statistics of the recent human sample, and results of the *z*-score analysis between the fossil sample and recent humans.[a]

Variable	Sima de los Huesos		Neandertals			Modern human males				
	VT6	VT29	Kebara 2	Shanidar 2	Shanidar 3	Mean	SD	Min	Max	*n*
Maximum dorso-ventral diameter (MaxDVDi)	**83.0***	(75.0)	67.2		(78.6)	73.19	3.89	62.6	81.9	55
Maximum transverse diameter (MaxTrDi)	(57.0)		43.1			47.35	4.99	35.2	58.8	57
Canal dorso-ventral diameter (M10)	17.7		19.4		17.4	17.39	1.34	13.3	20.5	64
Canal transverse diameter (M11)	20.6	17.4	18.9	20.2	18.9	20.35	1.73	16.7	26.2	64
Spinous process: maximum length (M13)	**37.1***	36.1	28.0	29.1	(35.0)	30.69	2.93	23.9	36.9	51

[a]Values in parentheses are estimated. Values underlined are outside the range of the modern human comparative sample. The values with a * or two ** are significantly different from the modern male comparative sample (* = $p < 0.05$, ** = $p < 0.01$). Values in bold indicate those values that are significantly different and/or outside of the range of the modern human sample.
Source: Data from Gómez-Olivencia (2009).

that is, *z*-score values beyond 1.96 ($p < 0.05$) and 2.576 ($p < 0.01$) standard deviations (Sokal & Rohlf, 1981) and/or beyond the range of our modern comparative sample were highlighted. Bivariate plots were performed in the R statistical environment (R Core Team, 2016).

TABLE 4 Inventory of selected and most complete adult ribs from Sima de los Huesos.

Anatomical position and side[a]	Label	Field label	Description	Figure
1R	–	AT-2600	Partial first rib: it preserves the head, the neck, the tubercle and c. half of the shaft.	Figure 4
1L	–	AT-3644 + AT-3665	Partial first rib: it preserves the head, the neck, the tubercle and c. half of the shaft.	–
1L	Co1	AT-2748 + AT-3546 + AT-3549	Almost complete first rib: it only lacks the head and part of the rib body.	Figure 4
2R	–	AT-3591 + AT-3658	Partial second rib: preserves the head, the neck, the tubercle and part of the shaft.	Figure 5
2L	–	AT-2987 + AT-3083	Partial second rib: preserves a large portion of the shaft and the sternal end	Figure 5
2R	–	AT-6115	Shaft portion.	Figure 5
3-4R	–	AT-797 + AT-3526 + AT-4814	Partial rib preserving a shaft portion, including the posterior angle.	Figure 6
4-5?L	–	AT-1250 + AT-2629 + AT-2637 + AT-2661	Very complete upper-middle rib that preserves the head, the neck and a large part of the shaft, including the posterior angle. The tubercle area is almost completely eroded.	Figure 6
4–7R	–	AT-6297	Partial upper-middle rib, preserving part of the head, the neck, the tubercle and a small portion of the shaft.	Figure 6
5-7L	–	AT-1238 + AT-2626	Partial middle rib preserving a large portion of the shaft, including the posterior angle.	Figure 6
6-7R	–	AT-2635 + AT-2881 + AT-4347 + AT-5300	Partial middle rib preserving a large portion of the shaft, including the posterior angle.	Figure 6
7-9L	–	AT-3607 + AT-3639 + AT-3868	Partial middle rib preserving a large portion of the shaft, including the posterior angle.	-
8?L	–	AT-3869 + AT-3873 + AT-5686 + AT-5797 (8?R).	Partial middle-lower rib preserving a large portion of the shaft, including the posterior angle.	Figure 6
8-9?L	–	AT-1235 + AT-1249	Partial middle-lower rib preserving a large portion of the shaft, including the posterior angle.	Figure 6
9-10?L	–	AT-1237 + AT-2663	Partial lower rib preserving part of the tubercle and a large portion of the shaft, including the posterior angle.	Figure 6
11L	–	AT-1236 + AT-1246	Partial eleventh rib preserving approximately the sternal half of the shaft.	Figure 6
11R	Co3	AT-2624 + AT-2625 + AT-2639 + AT-6143	Nearly complete eleventh rib that only lacks the head.	Figure 6
11R	–	AT-3867	Partial eleventh rib, preserving the head and approximately the half of the shaft.	–
12L	Co2	AT-3626 + AT-3627 + AT-3634 + AT-3642	Nearly complete twelfth rib that only lacks the head and the sternal end.	Figure 7
12L	–	AT-2638 + AT-6056	Partial twelfth rib preserving a large portion of the shaft	Figure 7
12R	–	AT-2631 + AT-2666	Nearly complete twelfth rib that only lacks the head and the vertebral-most portion of the shaft.	Figure 7
12R	Co5	AT-6191 + AT-6676 + AT-6694 + AT-6715	Complete twelfth rib.	Figure 7

[a]L = left; R = right.

3 | RESULTS

3.1 | The thoracic spine

The SH sample contains 335 fragments that represent a minimum of 95 thoracic vertebrae. The most complete adult thoracic vertebrae are listed in Table 1. Selected adult thoracic vertebrae from SH are shown in Figures 1–3. Given the difficulty to establish the exact anatomical determination for thoracic vertebrae, this study is restricted to the first (T1) and twelfth (T12) thoracic vertebrae.

3.1.1 | The first thoracic vertebra (T1)

Selected first thoracic vertebrae (T1s) from SH are shown in Figure 1. The general dimensions of the most complete

FIGURE 4 Selected most complete first ribs from Sima de los Huesos. Cranial (a) and caudal (b) views of AT-2600(1R). Cranial (c) and caudal (d) views of Co1 (1L).

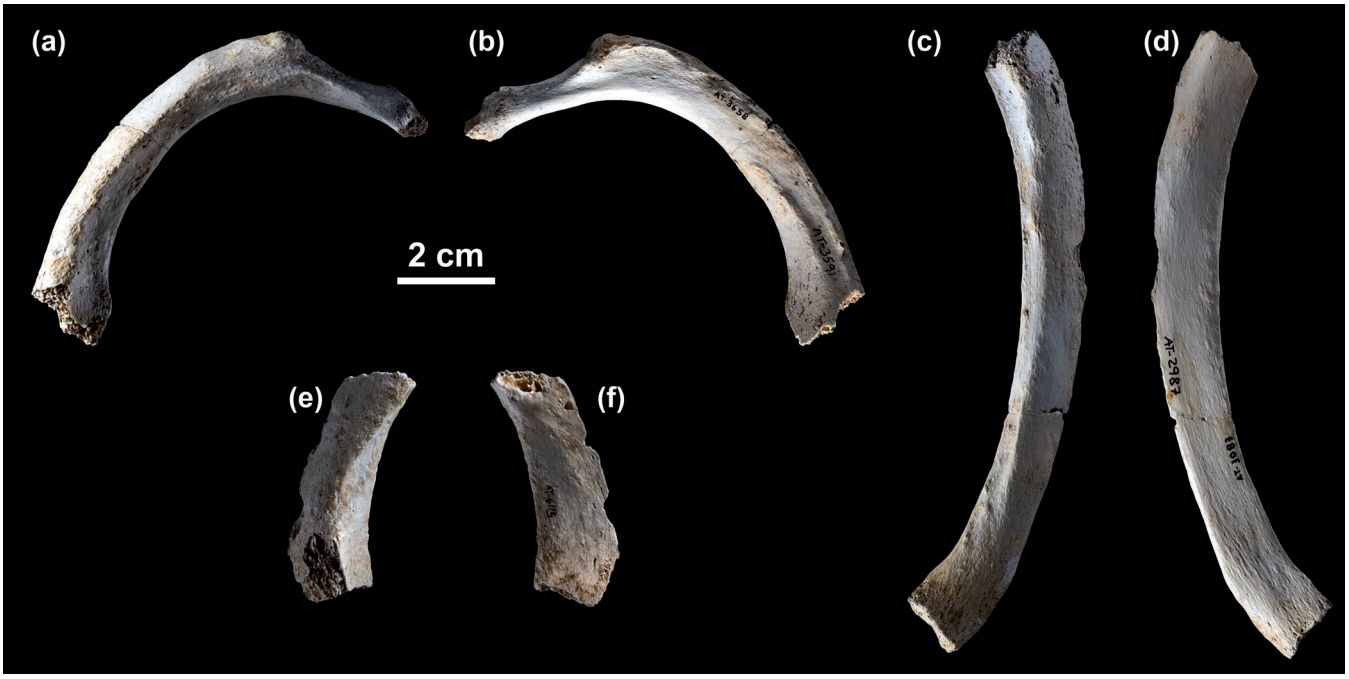

FIGURE 5 Selected adult second ribs from Sima de los Huesos. Cranial (a) and caudal (b) views of AT-3591 + AT-3658(2R). Cranial (c) and caudal (d) views of AT-2987 + AT-3083(2L). Cranial (e) and caudal (f) views of AT-6115(2R). R = right; L = Left.

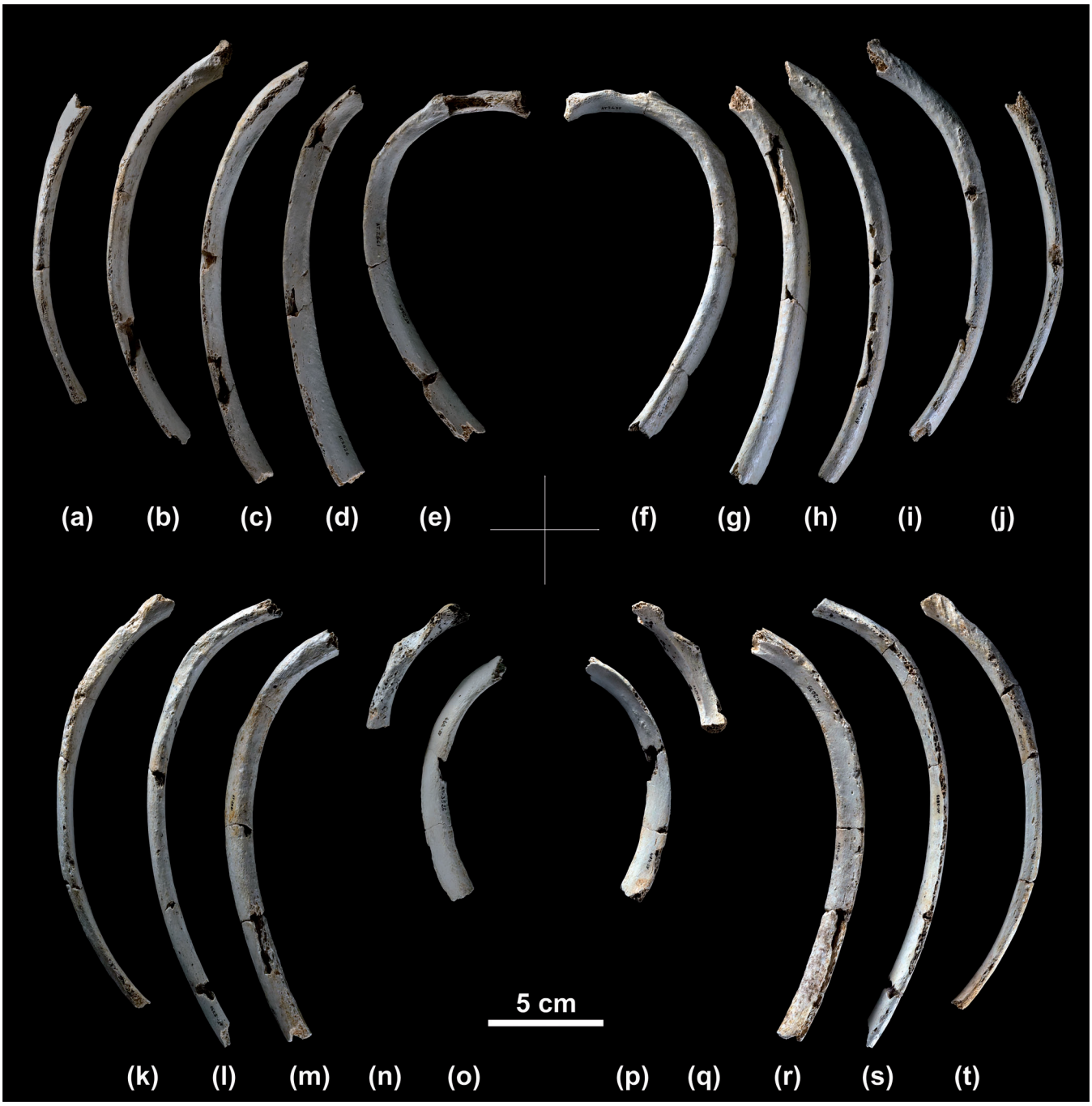

FIGURE 6 Selected adult ribs from the left (top) and right (bottom) sides from Sima de los Huesos in cranial and caudal views. Caudal (a) and cranial (j) views of AT-1236 + AT-1246(11L). Caudal (b) and cranial (i) views of AT-1237 + AT-2663(9-10?L). Caudal (c) and cranial (h) views of AT-1235 + AT-1249(8-9?L). Caudal (d) and cranial (g) views of AT-1238 + AT-2626(5-7L). Caudal (e) and cranial (f) views of AT-1250 + AT-2629 + AT-2637 + AT-2661(4-5?). Cranial (k) and caudal (t) views of Co3(11R). Cranial (l) and caudal (s) views of AT-3869 + AT-3873 + AT-5686 + AT-5797(8?R). Cranial (m) and caudal (r) views of AT-2635 + AT-2881 + AT-4347 + AT-5300(6-7R). Cranial (n) and caudal (q) views of AT-6297(4-7R). Cranial (o) and caudal (p) views of AT-797 + AT-3526 + AT-4814(3-4R).

T1s from SH fall well within our modern human comparative sample (Table 2). In the cases of VT12, when compared to our Euroamerican female sample, it is at the upper ends for both the maximum dorso-ventral diameter and the maximum transverse diameter (Table 1). The SH T1s show laterally oriented transverse processes and dorsally facing upper articular facets, similar to Neandertals and *H. sapiens*. The SH T1s show laterally oriented transverse processes and dorsally facing upper articular facets, similar to Neandertals and *H. sapiens*, whereas the

FIGURE 7 Selected most complete twelfth ribs from Sima de los Huesos. Cranial (a), external (b) and caudal (c) views of Co2(12L). Cranial (d), external (e) and caudal (f) views of AT-2631 + AT-2666 (12R). Cranial (g), external (h) and caudal (i) views of AT-2638 + AT-6056 (12L). Cranial (j), external (j) and caudal (l) views of Co5(12R). The arrow with a "1" indicates a hollow to accommodate the transverse process of the T12. The arrow with a "2" indicates the presence of two crests separated by a sulcus in the cranial aspect of the vertebral half of the shaft.

KNM-WT 15000 T1 (label: S) shows transverse processes oriented more dorsally and upper articular facets facing more medially (see Latimer & Ward, 1993). Finally, we hypothesize that the perceived size differences between VT12 and VT10 (and AT-3351) are due to sexual dimorphism, as has been observed in other postcranial regions in this collection (e.g., Arsuaga et al., 1997, 2015; Carretero et al., 2012; Lorenzo et al., 1998).

3.1.2 | The twelfth thoracic vertebra (T12)

Selected twelfth thoracic vertebrae (T12s) from SH are shown in Figure 3 and their preliminary metric comparison with Neandertals and *H. sapiens* is shown in Table 3. VT6 is significantly longer than our modern human comparative sample in both its maximum dorso-ventral dimension and the length of the spinous process; the former being a consequence of the latter. Additionally, the maximum transverse diameter of this vertebra is marginally significantly larger (z-score = 1.93; $0.05 < p < 0.10$) due to laterally projecting transverse processes, which are also present in VT29 (Figure 3). These projecting transverse processes are related to the narrowing of the costal shaft of the last ribs just sternal to the head, in order to accommodate this process (see below).

3.2 | The costal skeleton and the sternum

The SH sample contains 652 costal fragments that represent a minimum of 118 ribs. The most complete adult ribs are listed in Table 4. Selected adult ribs from SH are shown in Figures 4–7. Given the fragmentary status of most of the ribs, and the difficulty to establish the exact

anatomical position, this study is restricted to the first, the second and the twelfth ribs.

The SH sample contains 26 sternal fragments and a selection of the most complete are shown in Figure 8.

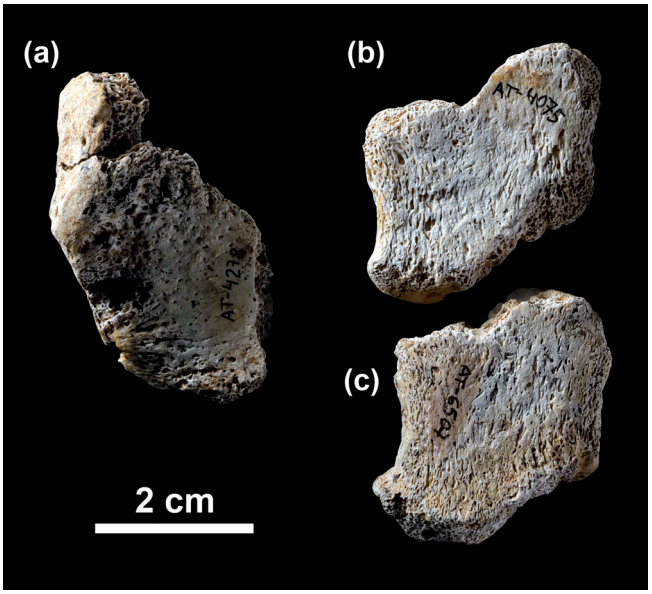

FIGURE 8 Ventral (anterior) views of selected most complete sternal elements from Sima de los Huesos. (a) the manubrium AT-4278, (b) the unfused sternebra AT-4075, (c) the unfused sternebra AT-6507, that likely refits with AT-4075.

The SH sternum collection is very fragmentary and does not currently allow a comparative study.

3.2.1 | The first rib

The two most complete adult ribs in the SH collection are shown in Figure 4, though only one of them is complete. This rib shows a very long dorso-ventral diameter which is significantly larger and outside the range of variation of our modern male sample (Table 5; Gómez-Olivencia, 2009; Arsuaga et al., 2015). Its tuberculo-ventral arc is close (approximately 1 standard deviation above) to that of the modern male sample. This results in a relatively straight shape for this rib, similar to the Regourdou 1 Neandertal (Figure 9; Gómez-Olivencia et al., 2010, 2019). A less curved morphology for the first rib of Neandertals has been proposed using different approaches, that is, both traditional (e.g., Gómez-Olivencia et al., 2019) and geometric morphometrics (Bastir et al., 2015).

3.2.2 | The second rib

Selected adult second ribs from SH are shown in Figure 5. Currently, no complete adult second rib is present in the SH collection. The vertebral half of the shaft in these ribs

TABLE 5 Dimensions (in mm) of the curvature of the complete first rib from Sima de los Huesos compared to both Neandertals and to the summary statistics of the recent human sample, and results of the *z*-score analysis between the fossil sample and recent humans.[a]

Sample/species	Individual/ label	Side	Tuberculo-ventral chord	Tuberculo-ventral arc	References
Sima de los Huesos	Co1	Left	**97.5****	(115.0)	Gómez-Olivencia, 2009; Arsuaga et al., 2015
Neandertals	Kebara 2	Right	85.7	99.0	Gómez-Olivencia et al., 2009
		Left	82.7	(96.0)	Gómez-Olivencia et al., 2009
	Regourdou 1	Right	94.2	103.0	Gómez-Olivencia et al., 2019
		Left	**92.8***	103.5	Gómez-Olivencia et al., 2019
	Sidrón SD-1767	Right	79.05	105.0	Bastir et al., 2015
	Sidrón SD-1699+	Left	(83.0)	(115.0)	Bastir et al., 2015
Modern humans (male)	Recent	Right	84.68 ± 5.42 (74.8–94.5) $n = 30$	104.24 ± 9.35 (85.0–126.0) $n = 30$	Gómez-Olivencia, 2009; Gómez-Olivencia et al., 2019
		Left	83.87 ± 4.52 (73.9–91.4) $n = 30$	104.38 ± 8.34 (86.0–120.0) $n = 30$	Gómez-Olivencia, 2009; Gómez-Olivencia et al., 2019

[a]Values in parentheses are estimated. Values underlined are outside the range of the modern human comparative sample. The values with a * or two ** are significantly different from the modern male comparative sample (* = $p < 0.05$, ** = $p < 0.01$). Values in bold indicate those values that are significantly different and/or outside of the range of the modern human sample.

shows a thick cranio-caudal dimension (>10 mm; Figure 5) which is significantly larger than the modern human comparative sample and is also thicker than the values of the second ribs of Kebara 2 (4.8 mm in both ribs) and Regourdou 1 (8.2 mm) (Figure 10; Gómez-Olivencia, 2009). This area is the insertion point of the *M. serratus posterior superior, M. scalenus posterior* and *M. serratus anterior*. These muscles arise from the spinous processes of the C7-T2, the posterior tubercles of the transverse processes of the caudalmost 2–3 cervical vertebrae (i.e., C5-C7 or C6-C7), and the anterior surface of the superior angle of the scapula, respectively. Gómez-Olivencia et al. (2009) compared the AT-2987 + AT-3083 specimen to the second rib of Kebara 2 and estimated the tubercle-ventral chord to be around 155 mm, which would be above the range of variation of our modern human comparative sample. The recent reconstruction of a nearly complete second rib of the Regourdou 1 individual led to the suggestion of a similar estimation for this variable for this individual (Gómez-Olivencia et al., 2019). The direct comparison of the AT-2987 + AT-3083 with the second rib of Regourdou 1 (Figure 10) suggests that the 155 mm should be regarded as a minimum value and that it is likely that AT-2987 + AT-3083 belonged to a dorsoventrally longer second rib than Kebara 2 and Regourdou 1.

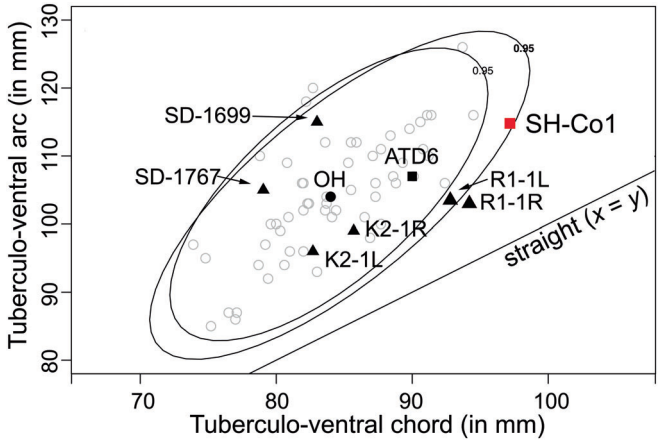

FIGURE 9 Bivariate plot representing the curvature of the 1st complete rib from Sima de los Huesos (Co1; red square) compared to Neandertals (black triangles), other fossil specimens (black squares or circles) and modern male humans (represented by gray open circles and 95% equiprobability ellipses). ATD6 represents the ATD6-108 1st right rib from Gran Dolina-TD6 level belonging to *Homo antecessor*. OH represents the Ohalo 2-H2 Upper Paleolithic modern human. Individuals closer to the straight ($x = y$) line represent straighter ribs. Modified from Gómez-Olivencia et al. (2010, 2019). L = Left; R = right; K2 = Kebara 2; R1 (Regourdou 1); SD = El Sidrón. The Sidrón (SD-) individuals are more similar to modern humans likely due to differences in measuring techniques.

3.2.3 | The twelfth rib

Selected adult twelfth ribs from SH are shown in Figure 7, including the complete rib Co5(12R). On the cranial edge of the vertebral half it is possible to observe

FIGURE 10 Cranial views of the adult second ribs from Sima de los Huesos compared to two Neandertals and to a modern human Euroamerican male. Sima de los Huesos: (a): AT-3591 + AT-3658(2R), (b): AT-6115(2R), and (f): AT-2987 + AT-3083(2L) (f). Neandertals: (c): Kebara 2 (2R) and (e): Regourdou 1 (2L). *Homo sapiens*: (d): Hamann-Todd collection (HTH-1533; 2R).

TABLE 6 Inventory of the most complete adult lumbar vertebrae from Sima de los Huesos.

Anatomical position	Label	Field label	Age-at-death	Brief description	Figure/ reference(s)
L1	VL16	AT-2592 + AT-2695 + AT-2707 + AT-4038 + AT-4906	Adult	Partial vertebra that preserves most part of the vertebral body, both pedicles, the upper left articular facet, the laminae, both lower articular facets and root of the spinous process.	–
L1	VL10	AT-875 + AT-1131 + AT-3010 + AT-3012	Adult	Nearly complete vertebra that only lacks the right transverse process	Figure 11
L2	VL1	AT-2590 + AT-2593 + AT-2693 + AT-2705 + AT-2706	Adult	Nearly complete vertebra which lacks a fragment of the vertebral body and the transverse processes.	–
L2?	VL18	AT-4188 + AT-5578 + AT-5673	Adult	Nearly complete vertebra except for both transverse processes and the upper right articular facet	Figure 11
L3	VL2	AT-2589 + AT-2591 + AT-2594 + AT-2657	Adult	Nearly complete vertebra that only lacks the left transverse process.	Figure 13
L3?	VL7	AT-866 + AT-4224 + AT-6173	Adult	Nearly complete vertebra that only lacks both transverse processes.	Figure 11
L4	VL3	AT-2588 + AT-2658	Adult	Nearly complete vertebra that only lacks both transverse processes.	–
L4	VL4	AT-3730 + AT-3731	Adult	Partial vertebra that preserves the vertebral body, the pedicle, both articular facets, and the lamina from the left side and the root of the spinous process.	–
L5	VL5	AT-1128 + AT-2659 + AT-6055	Adult	Nearly complete vertebra that only lacks the right transverse process.	Figure 12
L5	VL12	AT-3337 + AT-3728 + AT-3732 + AT-3740 + AT-3848 + AT-5687	Adult	Nearly complete vertebra that only lacks the right transverse process and part of the right lower articular facet.	Figure 12
L5	VL13	AT-1129 + AT-1225 + AT-3980	Adult	Very complete vertebra that lacks the transverse processes, the lower articular facet and lamina from the left side and the spinous process.	Figure 11

Note: VL16(L1), VL1(L2), VL2(L3), VL3(L4) and VL5(L5) are associated with Pelvis 1 (Bonmatí et al., 2010).

two crests with a sulcus between them. This feature was firstly described by Franciscus and Churchill (2002) in the 12th ribs of Shanidar 3 as the insertion points for the internal and external intercostal muscles and have been also observed in Kebara 2 and Regourdou 1 individuals (Gómez-Olivencia et al., 2019). However, the most noticeable feature of the twelfth ribs from SH is the narrowing of the shaft just sternal to the head. Based on our observations of the transverse processes of the T12 vertebrae, we consider that this narrowing accommodates the laterally projecting transverse processes of the T12 vertebrae.

3.3 | The lumbar spine

The SH sample contains 175 lumbar fragments that represent a minimum of 47 lumbar vertebrae. The most complete adult lumbar vertebrae are listed in Table 6. Selected lumbar vertebrae from SH are shown in Figure 11. Previous studies have detected differences between Neandertals and modern humans in the estimated degree of lumbar lordosis, the size of the vertebral foramen in L4-L5, and the length and orientation of the transverse processes.

The lumbar lordosis (LL) of the SH hominins was calculated to be between 23° and 35° by Been et al. (2014) based on the pelvic incidence values of Pelvis 1 (28°) and Pelvis 2 (33°) published by Bonmatí et al. (2010). These values, similar to that published for other Neandertal specimens (Table 7; but see Haeusler et al., 2019), are 10–15° lower than the Paleolithic *H. sapiens* Ohalo II H2 and significantly below a modern human sample. Currently, it is not possible to estimate the lumbar lordosis of the SH hominins based on other methods that quantify the lumbar vertebral morphology. On the one hand, the most complete association of lumbar vertebrae from SH, that is, those associated to Pelvis 1, are pathological (Bonmatí

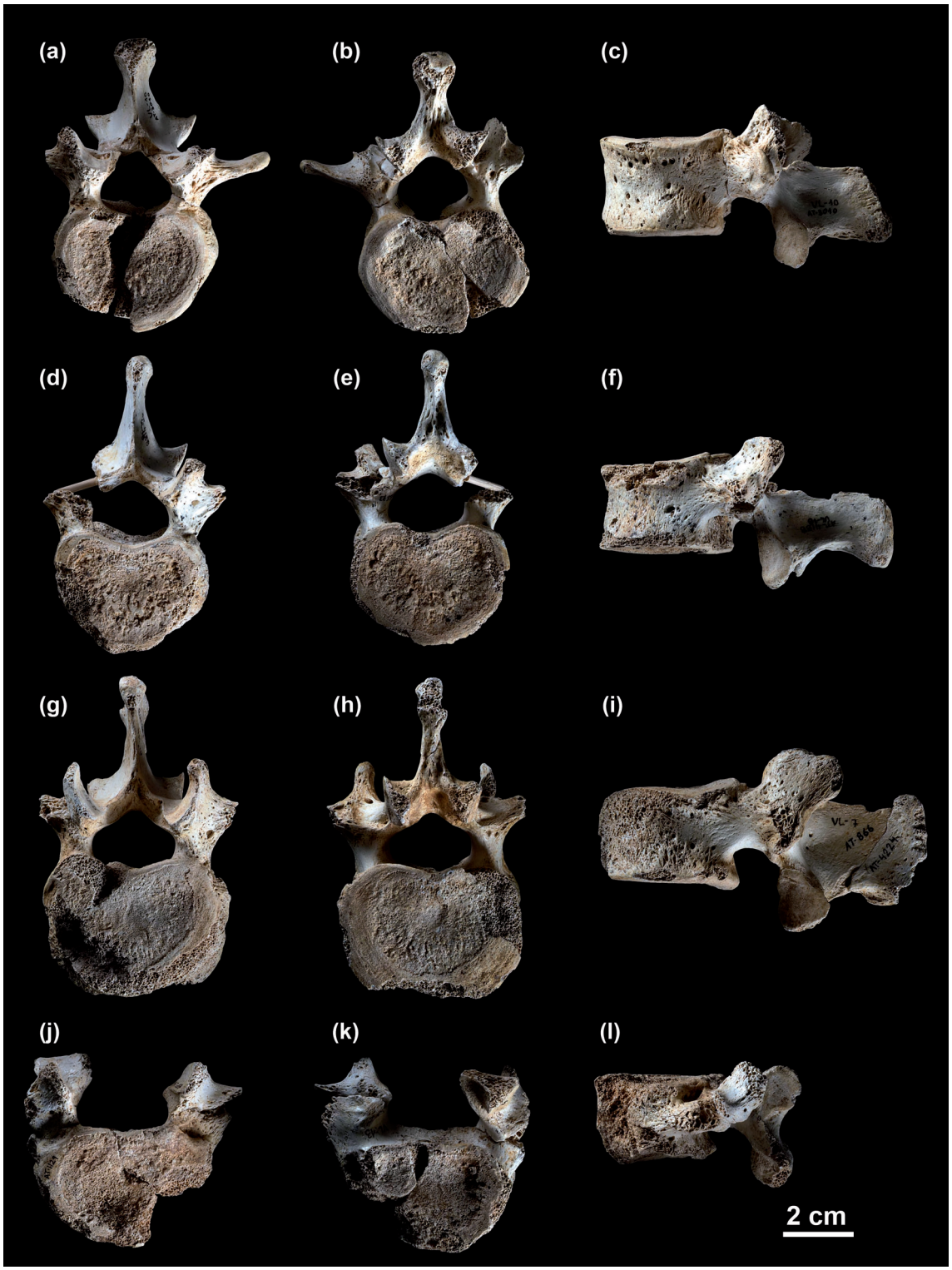

FIGURE 11 Selected lumbar vertebrae from Sima de los Huesos. Cranial (a), caudal (b) and left lateral (c) views of the VL10(L1). Cranial (d), caudal (e) and left lateral (f) views of the VL18 (L2?). Cranial (g), caudal (h) and left lateral (i) views of the VL7(L3?). Cranial (j), caudal (k) and left lateral (l) views of the VL13(L5).

et al., 2010) and the abnormal wedging would underestimate the actual LL value. On the other hand, no other association between lumbar vertebrae has been conducted yet that would allow the independent assessment of LL. Additional SH specimens and Paleolithic *H. sapiens* would be necessary to confirm this

TABLE 7 Lumbar lordosis angle in hominins.

	Mean group lordosis based on articular process[a]	Mean group lordosis based on pelvic incidence[b]
Australopithecus spp.	41 ± 4 ($n = 2$)	40 ± 5.9
		Range: 33.5[c]–45 ($n = 3$)
H. erectus	45 ($n = 1$)	45.5 ± 0 ($n = 2$)
Sima de los Huesos		29.5 ± 2.8 ($n = 2$)
H. neanderthalensis	29 ($n = 3$)	32.5
Fossil *H. sapiens*	54 ± 14 ($n = 2$)	48 ($n = 1$)
Modern *H. sapiens*	51.2 ± 11.1	
	Range: 32–78 ($n = 47$)	
Nonhuman hominoids	22.1 ± 3.2	
	Range: 18–28 ($n = 10$)	

[a]After Been et al., 2012.
[b]After Been et al., 2014. Mean of the two methods.
[c]Based on the reconstructed pelvis of MH2 (*A. sediba*).

perceived difference, especially given the differences found between the lordosis between preindustrial and postindustrial populations (Williams et al., 2022).

The studied L4 and L5 from SH have vertebral foramina that are close to the modern human means (Figure 12; Table 8). Neandertals show a different pattern in L4 and L5. In L4, the two complete specimens (Kebara 2 and La Chapelle-aux-Saints 1 -LC1-) show dorso-ventral and medio-lateral dimensions that are above the mean but within the range of variation of our modern human comparative sample and seem to follow the modern human pattern. In the case of L5, Neandertals show a very long canal in dorso-ventral dimension, and while some individuals (Shanidar 3, LC1) show very wide foramina in medio-lateral dimensions, other individuals (Kebara 2) do not.

Regarding the length of the transverse processes, the SH adult sample only preserves three complete transverse processes. Two of them are preserved in the L3 and L5 of the Pelvis 1 individual and the other is VL12 (L5). All of these transverse processes are above the range of variation of modern humans and also above the Neandertal sample (Bonmatí et al., 2010; Gómez-Olivencia et al., 2017).

The orientation of the transverse processes, in Neandertals is significantly different in L2-L4, in that they show very laterally oriented transverse processes. The orientation of the transverse process of the only vertebra in this anatomical range in SH is VL3, belongs to the Pelvis 1 individual. This specimen shows a dorso-lateral orientation, which is also present in the lumbar vertebrae of the KNM-WT 15000 *H. erectus* specimen and in *H. sapiens* (Figure 13).

4 | DISCUSSION AND CONCLUSIONS

Cautiously considering the restricted fossil record, and based on the most complete remains of the collection, the thorax and lumbar morphology of the SH hominins does not fully conform to the morphology present in Neandertals or in *H. sapiens*. Additionally, it also presents morphological differences with the restricted *H. erectus* fossil record. Table 9 presents a summary of the morphological features of the SH hominins compared to other species of the genus *Homo*.

First, regarding the thoracic spine, the SH hominins show laterally oriented transverse processes in T1, which is a derived condition in the genus *Homo*, shared with Neandertals and modern humans. We hypothesize that this feature appeared in the last common ancestor of modern humans and Neandertals. The morphology observed in the KNM-WT 15000 T1, assuming that the orientation of the transverse processes of this individual is representative of adult *H. erectus*, could be regarded as primitive within the genus *Homo*, based on the current fossil record. Therefore, it would be necessary to assess the first rib-first thoracic vertebra complex in order to better understand the consequences of perceived differences in this anatomical region.

Second, to our knowledge, the presence of laterally projecting transverse processes in the SH T12s and the related narrowing of the costal shaft in the last ribs is unique among extinct hominins. Both earlier species (*H. erectus*; KNM-WT 15000; see Haeusler et al., 2011; Bastir et al., 2020) and later species (modern humans and Neandertals; Gómez-Olivencia, Couture-Veschambre, et al., 2013; White & Folkens, 2005) normally show no transverse process (or a very reduced one) but a dorsally oriented projection slightly lateral and dorsal to the upper articular facets, that would correspond to the mammillary processes that the upper articular facets of the lumbar vertebrae bear. We hypothesize that this is an anatomical variation probably due to a shift in the expression of the HOX genes with no further consequence. We hypothesize that its presence in more than one individual could be related to the fact that this sample probably represents a single biological population with a certain degree of endogamy (Manzi et al., 2000 and references therein).

Third, regarding the thorax size and shape, based on the evolutionary position between *H. erectus* and

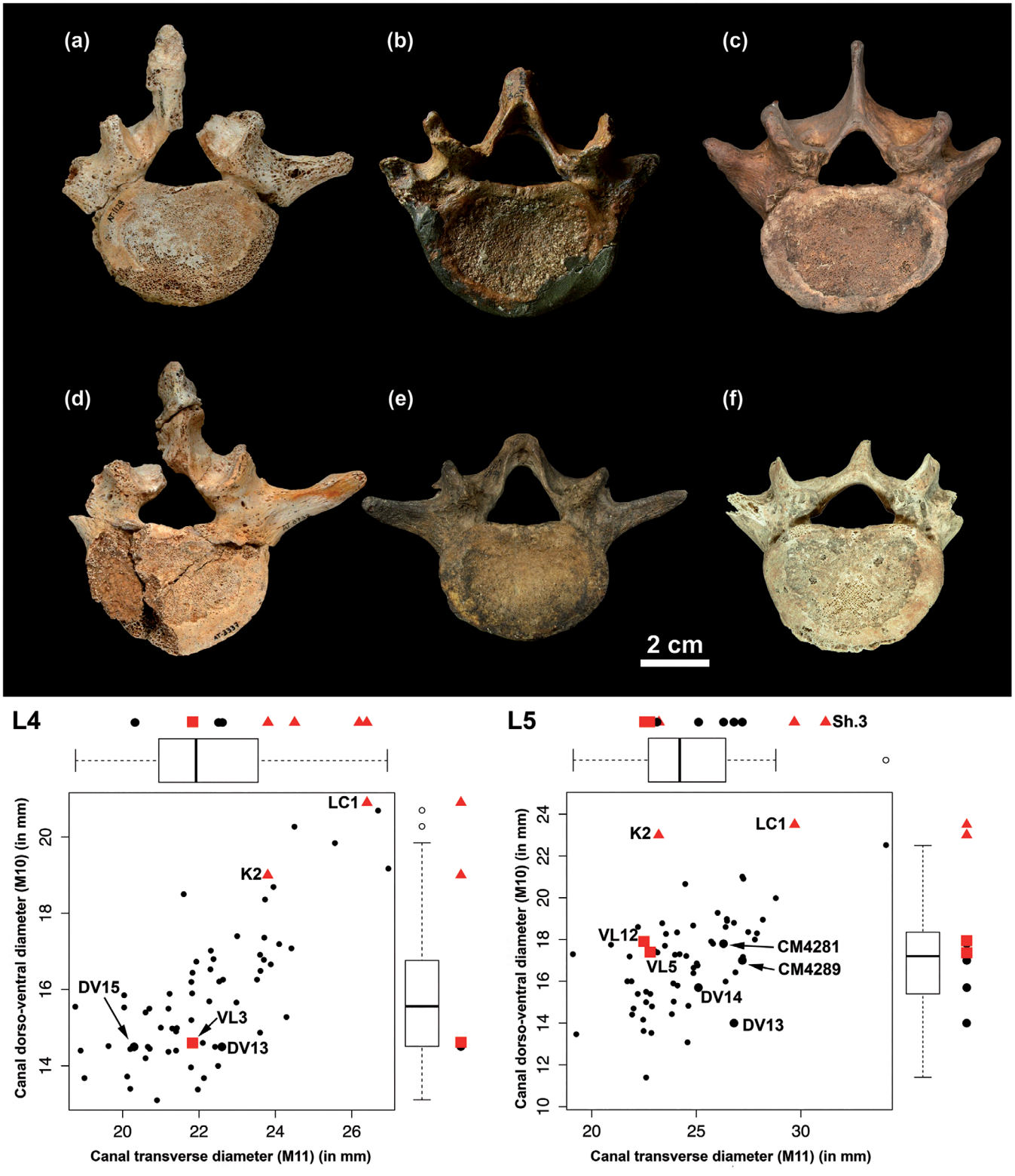

FIGURE 12 Top: Cranial views of two fifth lumbar vertebrae (L5) from Sima de los Huesos (SH) compared to two Neandertal and two *Homo sapiens* individuals. Sima de los Huesos: (a): VL5, and (d): VL12. Neandertals: (b) La Chapelle-aux-Saints 1 (LC1), and (e): Shanidar 3. *Homo sapiens*: (c): a recent European individual (I-B-19) from Burgos (University of Burgos) and (f): Cro-Magnon (CM4281). Bottom: bivariate and univariate plots of the vertebral foramen variables for L4 and L5. Black dots represent modern human individuals; larger black dots represent fossil modern humans; red triangles represent Neandertals; red squares represent the SH specimens. Box and whiskers represent the modern human univariate descriptive statistics (median, Q1, Q3, etc.) for each of the variables. Modified from Gómez-Olivencia et al. (2017).

TABLE 8 Dimensions (in mm) of the vertebral foramen of the most complete fourth (L4) and fifth lumbar (L5) vertebrae from Sima de los Huesos compared to both Neandertals and to the summary statistics of the recent human sample, and results of the *z*-score analysis between the fossil sample and recent humans.[a]

Vertebra	Sample/species	Individual/label	Canal dorso-ventral diameter (M10)	Canal transverse diameter (M11)	References
L4	Sima de los Huesos	VL3	14.6	21.8	Gómez-Olivencia, 2009; Bonmatí et al., 2010
	Neandertals	Kebara 2	19.0	23.8	Gómez-Olivencia et al., 2017
		La Chapelle-aux-Saints 1	**20.9****	**26.4***	Gómez-Olivencia et al., 2017
		La Ferrassie 1		25.5	Gómez-Olivencia et al., 2017
		Shanidar 3		24.5	Gómez-Olivencia et al., 2017
	Modern humans	Recent	15.84 ± 1.73 (13.1–20.7) $n = 59$	22.12 ± 1.75 (18.8–27.0) $n = 59$	Gómez-Olivencia et al., 2017
L5	Sima de los Huesos	VL5	17.2	22.8	Gómez-Olivencia, 2009; Bonmatí et al., 2010
		VL12	17.9	22.4	Gómez-Olivencia, 2009
	Neandertals	Kebara 2	**23.0****	23.2	Gómez-Olivencia et al., 2017
		La Chapelle-aux-Saints 1	**23.5****	**29.7***	Gómez-Olivencia et al., 2017
		La Ferrassie 1		26.2	Gómez-Olivencia et al., 2017
		Shanidar 3		**(31.2)****	Gómez-Olivencia et al., 2017
	Modern humans	Recent	16.96 ± 2.18 (11.4–22.5) $n = 57$	24.56 ± 2.54 (19.1–34.1) $n = 59$	Gómez-Olivencia et al., 2017

[a]Values in parentheses are estimated. Values underlined are outside the range of the modern human comparative sample. The values with a * or two ** are significantly different from the modern male comparative sample (* = $p < 0.05$, ** = $p < 0.01$). Values in bold indicate those values that are significantly different and/or outside of the range of the modern human sample.

Neandertals, we hypothesize that the SH thorax is morphologically different from that of modern humans and more similar to *H. erectus* and Neandertals. This would be consistent with: (a) the perceived differences observed in the curvature of the first rib, which have been related by Bastir et al. (2015) to the whole thorax; and (b) the distinct SH pelvic morphology (Arsuaga et al., 1999, 2015; Bonmatí et al., 2010), and the covariation of the pelvis with the thoracic morphology (Torres-Tamayo et al., 2020) to the proposed models for the evolution of the body shape in the Neandertal and *H. sapiens* lineages (Arsuaga, 2010; Arsuaga et al., 1999, 2015; Carretero et al., 2004). However, the direct comparison of isolated elements such as the first rib or the partial second rib suggest that the thorax of some SH individuals might have been larger than Neandertal individuals such as Regourdou 1 or Kebara 2. The available evidence from SH reinforces the notion that the *H. sapiens* thorax is derived within genus *Homo* (see Bastir et al., 2020; Gómez-Olivencia et al., 2018, and references therein).

Fourth, the lumbar region of the SH hominins displays some shared apomorphies with Neandertals, but not the full suite of Neandertal-derived features. However, some of the differences observed in the SH sample could be related to the larger (especially in the medio-lateral dimension) body size of these hominins. We consider that the Neandertal lineage displays, as a derived feature, a somehow smaller curvature of the lumbar spine compared to the earlier hominins. However, the orientation of the transverse processes in the mid-lumbar spine in SH, based on a very restricted sample, seems to be primitive, and preserved in *H. sapiens*. Neandertals, however, show laterally oriented transverse processes in the mid-lumbar vertebrae, which could be regarded as a derived feature. Finally, we hypothesize that the longer transverse processes in SH and Neandertals could be related to the larger medio-lateral dimension of the pelvis in this lineage, and therefore, the smaller length of the *H. sapiens* transverse processes of the lumbar spine could be related to a narrower pelvis.

In summary, the SH hominins display a morphological pattern in their thorax and lumbar spine that is more similar to that of Neandertals than to recent (and fossil) *H. sapiens* populations, which is consistent with the

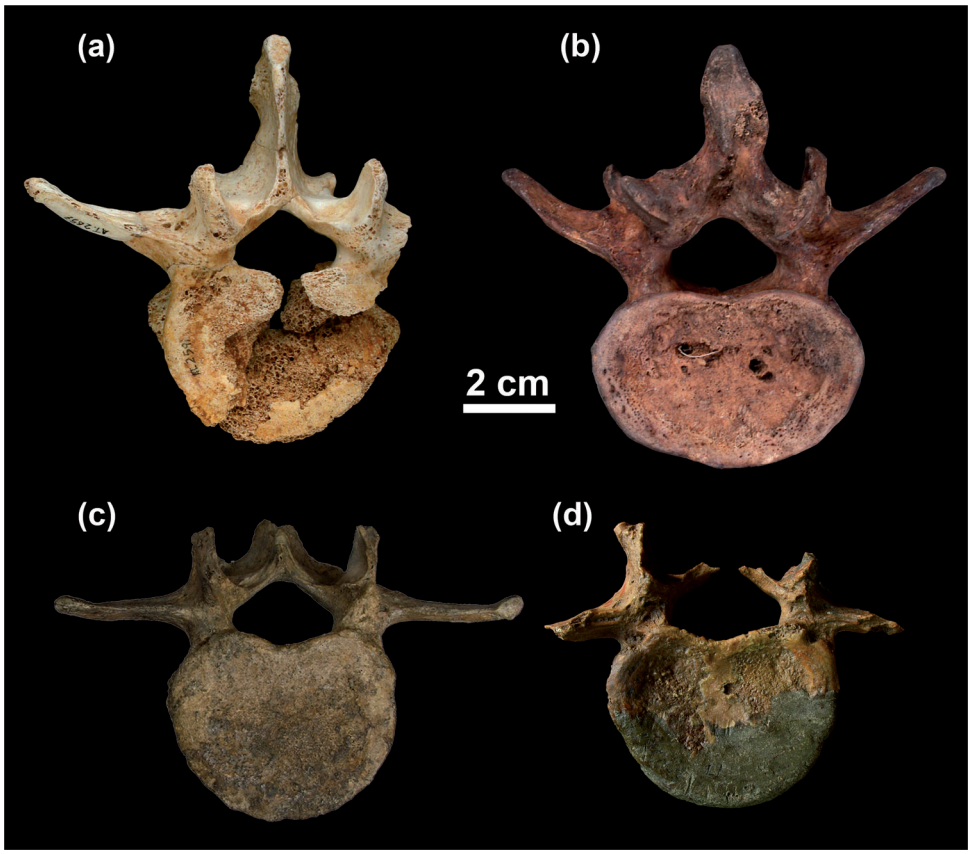

FIGURE 13 Comparison of the orientation of the transverse process of the third lumbar vertebra (L3) in cranial view. Sima de los Huesos: (a): VL2(L3), which belongs to the Pelvis 1 individual. *Homo sapiens*: (b) I-B-10 individual from Burgos (University of Burgos). Neandertals: (c): Kebara 2, and (d): La Chapelle-aux-Saints 1 individuals.

TABLE 9 The Neandertal vertebral and costal skeleton: summary of metrical and morphological traits.[a]

Bone	Trait	*H. erectus*	Sima de los Huesos	Neandertals	Modern *H. sapiens*	References
Thoracic spine	Orientation of the T1 transverse processes	Dorso-lateral	Lateral	Wider	Narrower	Latimer & Ward, 1993; Gómez-Olivencia et al., 2013a
Lumbar spine	Degree of lordosis of the lumbar spine	Low	Very low	Very low	Normal/Low[b]	Gómez-Olivencia, 2009; Bonmatí et al., 2010; Been et al., 2012, 2014
	Length of the transverse process		Very long	Long	Short	Been, 2005; Gómez-Olivencia, 2009; Gómez-Olivencia et al., 2017
	Transverse process orientation in cranial view (L2-L3)		Dorso-lateral	Lateral	Dorso-lateral	Been et al., 2010; Arsuaga et al., 2010; Gómez-Olivencia et al., 2017
	Vertebral canal dorso-ventral diameter (L5)		Normal	Dorsoventrally expanded	Normal	Been et al., 2010; Gómez-Olivencia et al., 2017
Costal skeleton	Shape of the first rib		Dorsoventrally expanded	Dorsoventrally expanded	Normal	Bastir et al., 2015
	Shaft of the second rib		Very robust	Robust	Normal	Gómez-Olivencia et al., 2009; Gómez-Olivencia, 2015

[a]Note that modern humans have been taken as the standard for most of these features, though this is not related to the polarity of the traits (see text).
[b]Note that the recent analysis by Williams et al. (2022) indicate a lower degree of lordosis in preindustrial *H. sapiens* populations when compared with postindustrial populations (see main text).

phylogenetic position of these hominins. These similarities encompass both the retention of primitive features in the Neandertal lineage and the presence of shared apomorphies. However, the SH hominins do not display the full suite of Neandertal-derived features in the studied regions, which is consistent with the studies of the cranium and postcranium of this deme. In order to fully comprehend the evolution of these anatomical regions in the genus *Homo*, apart from new fossil remains, additional studies are necessary to understand the morphological integration of the individual vertebrae, and their covariation with adjacent anatomical regions, such as the ribs and the pelvis.

AUTHOR CONTRIBUTIONS

Asier Gómez-Olivencia: Conceptualization; formal analysis; investigation; methodology; supervision; writing – original draft; writing – review and editing. **Juan Luis Arsuaga:** Project administration; funding acquisition; supervision; writing – review and editing.

ACKNOWLEDGMENTS

This study has been possible owing to the work and passion that the Sima de los Huesos excavation and research team has put in the excavation, curation, and research of this exceptional site for more than 30 years. We express our gratitude to the team. We thank Maicu Ortega for her work in restoring the fossils. Our acknowledgment and gratitude to Javier Trueba for the extraordinary graphic documentation of the SH fossils and fieldwork under very demanding conditions. We thank the following individuals and their institutions for granting us access to modern and fossil comparative materials: J.M. Carretero (Universidad de Burgos), P. Mennecier, A. Froment, D. Grimaud-Hervé, V. Laborde, A. Fort, L. Huet (Muséum national d'Histoire naturelle), V. Merlin-Anglade (Musée d'Art et d'Archeologie du Perigord, Périgueux), J.-J. Cleyet-Merle, S. Madelaine (Musée national de Prehistoire), Y. Haile-Selassie, B. Latimer, L. Jellema (Cleveland Museum of Natural History), R. G. Franciscus (University of Iowa), Y. Rak and I. Hershkowitz (Tel Aviv University). Further, we express our gratitude to the editors and the invited editors for the kind invitation to submit this manuscript. We benefited from fruitful discussions with our colleagues from the Centro UCM-ISCIII Sobre Evolución y Comportamiento Humanos of Madrid and the Laboratorio de Evolución Humana, at the University of Burgos, the IPHES and Universitat Rovira i Virgili, the Centro Nacional de Investigación sobre Evolución Humana (CENIEH, Burgos). We have also benefited from discussions about the anatomy and evolution of the spine and thorax with J.M. Carretero, E. Been, R. G. Franciscus, M. Arlegi, M. Meyer, M. Bastir, S. Williams, D. García-Martínez, T. Holliday, F. Jaeger, S. Madelaine, C. Couture, B. Maureille. This study was supported by the Spanish Ministerio de Ciencia, Innovación y Universidades (Projects PGC2018-093925-B-C33, MCI/AEI/FEDER, UE and PID2021-122355NB-C31, MCIN/AEI/10.13039/501100011033/FEDER, UE). Asier Gómez-Olivencia is supported by Ramón y Cajal fellowship (RYC-2017-22558). Field work in Atapuerca is supported by the Junta de Castilla y León and Fundación Atapuerca. We express our gratitude to the Editor, the AE, to Marc Meyer and an additional reviewer for very useful comments that have helped us improve this article.

ORCID

Asier Gómez-Olivencia https://orcid.org/0000-0001-7831-3902
Juan Luis Arsuaga https://orcid.org/0000-0001-5361-2295

REFERENCES

Aiello, L., & Dean, C. (1990). *An introduction to human evolutionary anatomy*. Academic Press.

Arlegi, M., Gómez-Olivencia, A., Albessard, L., Martínez, I., Balzeau, A., Arsuaga, J. L., & Been, E. (2017). The role of allometry and posture in the evolution of the hominin subaxial cervical spine. *Journal of Human Evolution*, *104*, 80–99.

Arlegi, M., Veschambre-Couture, C., & Gómez-Olivencia, A. (2020). Evolutionary selection and morphological integration in the vertebral column of modern humans. *American Journal of Physical Anthropology*, *171*, 17–36.

Arsuaga, J. L. (2010). Terrestrial apes and phylogenetic trees. *Proceedings of the National Academy of Sciences of the United States of America*, *107*, 8910–8917.

Arsuaga, J. L., Carretero, J.-M., Lorenzo, C., Gómez-Olivencia, A., Pablos, A., Rodríguez, L., García-González, R., Bonmatí, A., Quam, R. M., Pantoja-Pérez, A., Martínez, I., Aranburu, A., Gracia-Téllez, A., Poza-Rey, E., Sala, N., García, N., Alcázar de Velasco, A., Cuenca-Bescós, G., Bermúdez de Castro, J. M., & Carbonell, E. (2015). Postcranial morphology of the middle Pleistocene humans from Sima de los Huesos, Spain. *Proceedings of the National Academy of Sciences of the United States of America*, *112*, 11524–11529.

Arsuaga, J. L., Carretero, J. M., Lorenzo, C., Gracia, A., Martínez, I., Bermúdez de Castro, J. M., & Carbonell, E. (1997). Size variation in Middle Pleistocene humans. *Science*, *277*, 1086–1088.

Arsuaga, J. L., Lorenzo, C., Carretero, J. M., Gracia, A., Martínez, I., García, N., Bermúdez de Castro, J. M., & Carbonell, E. (1999). A complete human pelvis from the Middle Pleistocene of Spain. *Nature*, *399*, 255–258.

Arsuaga, J. L., Martínez, I., Arnold, L. J., Aranburu, A., Gracia-Téllez, A., Sharp, W. D., Quam, R. M., Falguères, C., Pantoja-Pérez, A., Bischoff, J., Poza-Rey, E., Parés, J. M., Carretero, J. M., Demuro, M., Lorenzo, C., Sala, N., Martinón-Torres, M., García, N., Alcázar de Velasco, A., ... Carbonell, E. (2014). Neandertal roots: Cranial and chronological evidence from Sima de los Huesos. *Science*, *344*, 1358–1363.

Bastir, M., García Martínez, D., Rios, L., Higuero, A., Barash, A., Martelli, S., García Tabernero, A., Estalrrich, A., Huguet, R., de la Rasilla, M., & Rosas, A. (2017). Three-dimensional morphometrics of thoracic vertebrae in Neandertals and the fossil evidence from El Sidrón (Asturias, northern Spain). *Journal of Human Evolution*, *108*, 47–61.

Bastir, M., García-Martínez, D., Estalrrich, A., García-Tabernero, A., Huguet, R., Ríos, L., Barash, A., Recheis, W., de la Rasilla, M., & Rosas, A. (2015). The relevance of the first ribs of the El Sidrón site (Asturias, Spain) for the understanding of the Neandertal thorax. *Journal of Human Evolution*, *80*, 64–73.

Bastir, M., García-Martínez, D., Torres-Tamayo, N., Palancar, C. A., Beyer, B., Barash, A., Villa, C., Sanchis-Gimeno, J. A., Riesco-López, A., Nalla, S., Torres-Sánchez, I., García-Río, F., Been, E., Gómez-Olivencia, A., Haeusler, M., Williams, S. A., & Spoor, F. (2020). Rib cage anatomy in *Homo erectus* suggests a recent evolutionary origin of modern human body shape. *Nature Ecology & Evolution*, *4*, 1178–1187.

Bastir, M., García-Martínez, D., Torres-Tamayo, N., Sanchis-Gimeno, J. A., O'Higgins, P., Utrilla, C., Torres Sánchez, I., & García Río, F. (2017). In vivo 3D analysis of thoracic kinematics: Changes in size and shape during breathing and their implications for respiratory function in recent humans and fossil hominins. *The Anatomical Record*, *300*, 255–264.

Been, E. (2005). The anatomy of the lumbar spine of *Homo neanderthalensis* and its phylogenetic and functional implications, Tel Aviv University.

Been, E., Gómez-Olivencia, A., & Kramer, P. A. (2012). Lumbar lordosis of extinct hominins. *American Journal of Physical Anthropology*, *147*, 64–77.

Been, E., Gómez-Olivencia, A., & Kramer, P. A. (2014). Brief communication: Lumbar lordosis in extinct hominins: Implications of the pelvic incidence. *American Journal of Physical Anthropology*, *154*, 307–314.

Been, E., Gómez-Olivencia, A., Shefi, S., Soudack, M., Bastir, M., & Barash, A. (2017). Evolution of spinopelvic alignment in hominins. *The Anatomical Record*, *300*, 900–911.

Been, E., Peleg, S., Marom, A., & Barash, A. (2010). Morphology and function of the lumbar spine of the Kebara 2 Neandertal. *American Journal of Physical Anthropology*, *142*, 549–557.

Bonmatí, A., Gómez-Olivencia, A., Arsuaga, J. L., Carretero, J. M., Gracia, A., Martínez, I., Lorenzo, C., Bermúdez de Castro, J. M., & Carbonell, E. (2010). Middle Pleistocene lower back and pelvis from an aged human individual from the Sima de los Huesos site, Spain. *Proceedings of the National Academy of Sciences*, *107*, 18386–18391.

Boule, M. (1911–1913). L'homme fossile de la Chapelle aux Saints. *Annales de Paléontologie*, *6*, 111–172; *7*: 21–56, 85–192; *8*: 1–70.

Brown, F. H., Harris, J., Leakey, R., & Walker, A. (1985). Early *Homo erectus* skeleton from West Lake Turkana, Kenya. *Nature*, *316*, 788–792.

Carretero, J. M., Arsuaga, J. L., Martínez, I., Quam, R., Lorenzo, C., Gracia, A., & Ortega, A. I. (2004). Los humanos de la Sima de los Huesos (Sierra de Atapuerca) y la evolución del cuerpo en el género *Homo*. In E. Baquedano & S. Rubio (Eds.), *Miscelánea en homenaje a Emiliano Aguirre. Volumen III. Paleoantropología* (pp. 120–135). Museo arqueológico regional.

Carretero, J. M., Lorenzo, C., & Arsuaga, J. L. (1999). Axial and appendicular skeleton of *Homo antecessor*. *Journal of Human Evolution*, *37*, 459–499.

Carretero, J. M., Rodríguez, L., García-González, R., Arsuaga, J. L., Gómez-Olivencia, A., Lorenzo, C., Bonmatí, A., Gracia, A., Martínez, I., & Quam, R. (2012). Stature estimation from complete long bones in the Middle Pleistocene humans from the Sima de los Huesos, sierra de Atapuerca (Spain). *Journal of Human Evolution*, *62*, 242–255.

Franciscus, R. G., & Churchill, S. E. (2002). The costal skeleton of Shanidar 3 and a reappraisal of Neandertal thoracic morphology. *Journal of Human Evolution*, *42*, 303–356.

García-Martínez, D., Bastir, M., Gómez-Olivencia, A., Maureille, B., Golovanova, L., Doronichev, V., Akazawa, T., Kondo, O., Ishida, H., Gascho, D., Zollikofer, C. P. E., Ponce de León, M., & Heuzé, Y. (2020). Early development of the Neanderthal ribcage reveals a different body shape at birth compared to modern humans. *Science Advances*, *6*, eabb4377.

García-Martínez, D., Bastir, M., Huguet, R., Estalrrich, A., García-Tabernero, A., Ríos, L., Cunha, E., de la Rasilla, M., & Rosas, A. (2017). The costal remains of the El Sidrón Neanderthal site (Asturias, northern Spain) and their importance for understanding Neanderthal thorax morphology. *Journal of Human Evolution*, *111*, 85–101.

García-Martínez, D., Radovčić, D., Radovčić, J., Cofran, Z., Rosas, A., & Bastir, M. (2018). Over 100 years of Krapina: New insights into the Neanderthal thorax from the study of rib cross-sectional morphology. *Journal of Human Evolution*, *122*, 124–132.

García-Martínez, D., Torres-Tamayo, N., Torres-Sanchez, I., García-Río, F., & Bastir, M. (2016). Morphological and functional implications of sexual dimorphism in the human skeletal thorax. *American Journal of Physical Anthropology*, *161*, 467–477.

García-Martínez, D., Torres-Tamayo, N., Torres-Sánchez, I., García-Río, F., Rosas, A., & Bastir, M. (2018). Ribcage measurements indicate greater lung capacity in Neanderthals and Lower Pleistocene hominins compared to modern humans. *Communications Biology*, *1*, 117.

Gelb, D. E., Lenke, L. G., Bridwell, K. H., Blanke, K. M., & McEnery, K. W. (1995). An analysis of sagittal spinal alignment in 100 asymptomatic middle and older aged volunteers. *Spine*, *20*, 1351–1358.

Goh, S., Price, R. I., Leedman, P. J., & Singer, K. P. (1999). The relative influence of vertebral body and intervertebral disc shape on thoracic kyphosis. *Clinical Biomechanics*, *14*, 439–448.

Gomez-Olivencia, A. (2009). *Estudios paleobiológicos sobre la columna vertebral y la caja torácica de los humanos fósiles del Pleistoceno, con especial referencia a los fósiles de la Sierra de Atapuerca* (p. 553). Universidad de Burgos.

Gómez-Olivencia, A. (2015). The costal skeleton of the Neandertal individual of La Chapelle-aux-saints 1. *Annales de Paléontologie*, *101*, 127–141.

Gómez-Olivencia, A., Arlegi, M., Barash, A., Stock, J. T., & Been, E. (2017). The Neandertal vertebral column 2: The lumbar spine. *Journal of Human Evolution*, *106*, 84–101.

Gómez-Olivencia, A., & Arsuaga, J. L. (2024). The Sima de los Huesos cervical spine. *The Anatomical Record*. (in press). https://doi.org/10.1002/ar.25224

Gómez-Olivencia, A., Barash, A., Arlegi, M., García-Martínez, D., Kramer, P. A., Bastir, M., & Been, E. (2015). 3D virtual

reconstruction of the Kebara 2 thorax. *Proceedings of the European Society for the Study of Human Evolution*, *4*, 100.

Gómez-Olivencia, A., Barash, A., García-Martínez, D., Arlegi, M., Kramer, P., Bastir, M., & Been, E. (2018). 3D virtual reconstruction of the Kebara 2 Neandertal thorax. *Nature Communications*, *9*, 4387.

Gómez-Olivencia, A., Been, E., Arsuaga, J. L., & Stock, J. T. (2013). The Neandertal vertebral column 1: The cervical spine. *Journal of Human Evolution*, *64*, 608–630.

Gómez-Olivencia, A., Carretero, J. M., Lorenzo, C., Arsuaga, J. L., Bermúdez de Castro, J. M., & Carbonell, E. (2010). The costal skeleton of *Homo antecessor*: Preliminary results. *Journal of Human Evolution*, *59*, 620–640.

Gómez-Olivencia, A., Carretero, J. M., Arsuaga, J. L., Rodríguez-García, L., García-González, R., & Martínez, I. (2007). Metric and morphological study of the upper cervical spine from the Sima de los Huesos site (Sierra de Atapuerca, Burgos, Spain). *Journal of Human Evolution*, *53*, 6–25.

Gómez-Olivencia, A., Couture-Veschambre, C., Madelaine, S., & Maureille, B. (2013). The vertebral column of the Regourdou 1 Neandertal. *Journal of Human Evolution*, *64*, 582–607.

Gómez-Olivencia, A., Eaves-Johnson, K. L., Franciscus, R. G., Carretero, J. M., & Arsuaga, J. L. (2009). Kebara 2: New insights regarding the most complete Neandertal thorax. *Journal of Human Evolution*, *57*, 75–90.

Gómez-Olivencia, A., Franciscus, R. G., Couture-Veschambre, C., Maureille, B., & Arsuaga, J. L. (2012). The mesosternum of the Regourdou 1 Neandertal revisited. *Journal of Human Evolution*, *62*, 511–519.

Gómez-Olivencia, A., Holliday, T., Madelaine, S., Couture-Veschambre, C., & Maureille, B. (2019). The costal skeleton of the Regourdou 1 Neandertal. *Journal of Human Evolution*, *130*, 151–171.

Haeusler, M., Martelli, S. A., & Boeni, T. (2002). Vertebrae numbers of the early hominid lumbar spine. *Journal of Human Evolution*, *43*, 621–643.

Haeusler, M., Schiess, R., & Boeni, T. (2011). New vertebral and rib material point to modern bauplan of the Nariokotome *Homo erectus* skeleton. *Journal of Human Evolution*, *61*, 575–582.

Haeusler, M., Trinkaus, E., Fornai, C., Müller, J., Bonneau, N., Boeni, T., & Frater, N. (2019). Morphology, pathology, and the vertebral posture of the La Chapelle-aux-saints Neandertal. *Proceedings of the National Academy of Sciences*, *116*, 4923–4927.

Haile-Selassie, Y., Latimer, B. M., Alene, M., Deino, A. L., Gibert, L., Melillo, S. M., Saylor, B. Z., Scott, G. R., & Lovejoy, C. O. (2010). An early *Australopithecus afarensis* postcranium from Woranso-Mille, Ethiopia. *Proceedings of the National Academy of Sciences*, *107*, 12121–12126.

Hawks, J., Elliott, M., Schmid, P., Churchill, S. E., Ruiter, D. J. d., Roberts, E. M., Hilbert-Wolf, H., Garvin, H. M., Williams, S. A., Delezene, L. K., Feuerriegel, E. M., Randolph-Quinney, P., Kivell, T. L., Laird, M. F., Tawane, G., DeSilva, J. M., Bailey, S. E., Brophy, J. K., Meyer, M. R., … Berger, L. R. (2017). New fossil remains of *Homo naledi* from the Lesedi chamber, South Africa. *eLife*, *6*, e24232.

Heim, J.-L. (1976). Les Hommes fossiles de la Ferrassie. I. Le gisement. In *Les Squelettes Adultes (crâne et Squelette du Tronc)*. Masson.

Jackson, R. P., & Hales, C. (2000). Congruent spinopelvic alignment on standing lateral radiographs of adult volunteers. *Spine*, *25*, 2808–2815.

Jellema, L. M., Latimer, B., & Walker, A. (1993). The rib cage. In A. Walker & R. Leakey (Eds.), *The Nariokotome* Homo erectus *skeleton* (pp. 294–325). Harvard University Press.

Kapandji, I. A. (1974). The physiology of the joints. In *The trunk and vertebral column* (Vol. 3). Churchill Livingstone.

Latimer, B., & Ohman, J. C. (2001). Axial displasia in *Homo erectus* (abstract). *Journal of Human Evolution*, *40*, A12.

Latimer, B., & Ward, C. V. (1993). The thoracic and lumbar vertebrae. In A. Walker & R. Leakey (Eds.), *The Nariokotome* Homo erectus *skeleton* (pp. 266–293). Springer.

Lordkipanidze, D., Jashashvili, T., Vekua, A., Ponce de León, M. S., Zollikofer, C. P. E., Rightmire, G. P., Pontzer, H., Ferring, R., Oms, O., Tappen, M., Bukhsianidze, M., Agusti, J., Kahlke, R., Kiladze, G., Martinez-Navarro, B., Mouskhelishvili, A., Nioradze, M., & Rook, L. (2007). Postcranial evidence from early homo from Dmanisi, Georgia. *Nature*, *449*, 305–310.

Lorenzo, C., Carretero, J. M., Arsuaga, J. L., Gracia, A., & Martinez, I. (1998). Intrapopulational body size variation and cranial capacity variation in middle Pleistocene humans: The Sima de los Huesos sample (sierra de Atapuerca, Spain). *American Journal of Physical Anthropology*, *106*, 19–33.

Lü, Z. (1990). La découverte de l'homme fossile de Jing-Niu-Shan. Première étude. *L'Anthropologie (Paris)*, *94*, 899–902.

Manzi, G., Gracia, A., & Arsuaga, J.-L. (2000). Cranial discrete traits in the Middle Pleistocene humans from Sima de los Huesos (Sierra de Atapuerca, Spain). Does hypostosis represent any increase in "ontogenetic stress" along the Neanderthal lineage? *Journal of Human Evolution*, *38*, 425–446.

Martínez, I., & Arsuaga, J. L. (1997). The temporal bones from Sima de los Huesos Middle Pleistocene site (Sierra de Atapuerca, Spain). A phylogenetic approach. *Journal of Human Evolution*, *33*, 283–318.

Meyer, M., Arsuaga, J.-L., de Filippo, C., Nagel, S., Aximu-Petri, A., Nickel, B., Martínez, I., Gracia, A., Bermúdez de Castro, J. M., Carbonell, E., Viola, B., Kelso, J., Prüfer, K., & Pääbo, S. (2016). Nuclear DNA sequences from the Middle Pleistocene Sima de los Huesos hominins. *Nature*, *531*, 504–507.

Meyer, M. R. (2005). *Functional biology of the Homo erectus axial skeleton from Dmanisi*. University of Pennsylvania.

Meyer, M. R., & Williams, S. A. (2019). The spine of early Pleistocene *Homo*. In E. Been, A. Gómez-Olivencia, & P. A. Kramer (Eds.), *Spinal evolution: Morphology, function, and pathology of the spine in hominoid evolution* (pp. 153–183). Springer.

Morwood, M. J., Brown, P., Jatmiko, Sutikna, T., Wahyu Saptomo, E., Westaway, K. E., Awe Due, R., Roberts, R. G., Maeda, T., Wasisto, S., & Djubiantono, T. (2005). Further evidence for small-bodied hominins from the Late Pleistocene of Flores, Indonesia. *Nature*, *437*, 1012–1017.

Preuschoft, H. (2004). Mechanisms for the acquisition of habitual bipedality: Are there biomechanical reasons for the acquisition of upright bipedal posture? *Journal of Anatomy*, *204*, 363–384.

R Core Team. (2016). *R: A language and environment for statistical computing*. R Foundation for Statistical Computing. https://www.R-project.org/

Robinson, J. T. (1972). *Early hominid posture and locomotion*. The University of Chicago Press.

Sala, N., Martínez, I., Lorenzo, C., García, R., Carretero, J. M., Rodríguez, L., Gómez-Olivencia, A., Aranburu, A., García, N., Quam, R., Gracia, A., Ortega, M. C., & Arsuaga, J. L. (2024). Taphonomic skeletal disturbances in the Sima de los Huesos postcranial remains. *The Anatomical Record*. (In press). https://doi.org/10.1002/ar.25197

Sanders, W. J. (1998). Comparative morphometric study of the australopithecine vertebral series Stw-H8/H41. *Journal of Human Evolution*, *34*, 249–302.

Sawyer, G. J., & Maley, B. (2005). Neanderthal reconstructed. *The Anatomical Record (Part B: New Anatomist)*, *283B*, 23–31.

Schmid, P. (1983). Eine Rekonstruktion des Skelettes von A. L. 288-1 (Hadar) und deren Konsequenzen. *Folia Primatologica*, *40*, 283–306.

Schmid, P., Churchill, S. E., Nalla, S., Weissen, E., Carlson, K. J., de Ruiter, D. J., & Berger, L. R. (2013). Mosaic morphology in the thorax of *Australopithecus sediba*. *Science*, *340*, 1234598.

Schultz, A. H. (1961). Primatologia. In *Handbuch der primatenkunde*. S. Karger.

Sokal, R. R., & Rohlf, F. J. (1981). *Biometry*. W.H. Freeman and Company.

Torres-Tamayo, N., García-Martínez, D., Nalla, S., Barash, A., Williams, S. A., Blanco-Pérez, E., Mata Escolano, F., Sanchis-Gimeno, J. A., & Bastir, M. (2018). The torso integration hypothesis revisited in *Homo sapiens*: Contributions to the understanding of hominin body shape evolution. *American Journal of Physical Anthropology*, *167*, 777–790.

Torres-Tamayo, N., Schlager, S., García-Martínez, D., Sanchis-Gimeno, J. A., Nalla, S., Ogihara, N., Oishi, M., Martelli, S., & Bastir, M. (2020). Three-dimensional geometric morphometrics of thorax-pelvis covariation and its potential for predicting the thorax morphology: A case study on Kebara 2 Neandertal. *Journal of Human Evolution*, *147*, 102854.

Trinkaus, E. (1983). *The Shanidar Neandertals*. Academic Press.

Vallois, H. V., & de Félice, S. (1976). Le sternum néandertalien du Regourdou. Note complementaire. *Anthropologischer Anzeiger*, *35*, 229–235.

Ward, C. V., Nalley, T. K., Spoor, F., Tafforeau, P., & Alemseged, Z. (2017). Thoracic vertebral count and thoracolumbar transition in *Australopithecus afarensis*. *Proceedings of the National Academy of Sciences*, *114*, 6000–6004.

Weber, J., & Pusch, C. M. (2008). The lumbar spine in Neanderthals shows natural kyphosis. *European Spine Journal*, *17*, S327–S330.

Weinstein, K. J. (2008). Thoracic morphology in near eastern Neandertals and early modern humans compared with recent modern humans from high and low altitudes. *Journal of Human Evolution*, *54*, 287–295.

White, T. D., & Folkens, P. A. (2005). *The human bone manual*. Elsevier Academic Press, New York.

Williams, S. A. (2012). Placement of the diaphragmatic vertebra in catarrhines: Implications for the evolution of dorsostability in hominoids and bipedalism in hominins. *American Journal of Physical Anthropology*, *148*, 111–122.

Williams, S. A., García-Martínez, D., Bastir, M., Meyer, M. R., Nalla, S., Hawks, J., Schmid, P., Churchill, S. E., & Berger, L. R. (2017). The vertebrae and ribs of *Homo naledi*. *Journal of Human Evolution*, *104*, 136–154.

Williams, S. A., & Meyer, M. R. (2019). The spine of *Australopithecus*. In E. Been, A. Gómez-Olivencia, & P. A. Kramer (Eds.), *Spinal evolution: Morphology, function, and pathology of the spine in hominoid evolution* (pp. 125–151). Springer.

Williams, S. A., Zeng, I., Paton, G. J., Yelverton, C., Dunham, C., Ostrofsky, K. R., Shukman, S., Avilez, M. V., Eyre, J., Loewen, T., Prang, T. C., & Meyer, M. R. (2022). Inferring lumbar lordosis in Neandertals and other hominins. *PNAS Nexus*, *1*, pgab005.

How to cite this article: Gómez-Olivencia, A., & Arsuaga, J. L. (2024). The Sima de los Huesos thorax and lumbar spine: Selected traits and state-of-the-art. *The Anatomical Record*, 1–26. https://doi.org/10.1002/ar.25414